Role of hepatocyte NADPH Oxidase 4 in oxidative stress and DNA damage by genotype 1a hepatitis C virus

THESIS

Submitted in partial satisfaction of the requirements for the degree of

MASTER OF SCIENCE

in Quantitative and Systems Biology

by

Nicole Leanne Bidaud Corder

Thesis committee:

Professor Jinah Choi, Ph.D., Chair
Professor David M. Ojcius, Ph.D.
Professor Néstor J. Oviedo, Ph.D., D.V.M.

The Thesis of Nicole Leanne Bidaud Corder is approved and it is acceptable in quality and form for publication on microfilm and electronically:

_____

Dr. Jinah Choi, Chair

_____

Dr. David M. Ojcius

_____

Dr. Néstor J. Oviedo

UNIVERSITY OF CALIFORNIA, MERCED
2014

This thesis is dedicated to

Joseph Gerard Hilomen Ramos, M.S.

> "What is the most resilient parasite? Bacteria? A virus? An intestinal worm? An idea. Resilient... highly contagious. Once an idea has taken hold of the brain it's almost impossible to eradicate. An idea that is fully formed - fully understood - that sticks; right in there somewhere."
>
> -Cobb, *Inception*[1]

For your love and support over the years, and for understanding that I am a simple person with a complicated mind, I am eternally grateful. For reminding me that I am enough, I do enough, and I have enough. Thank you for sacrificing everything you were fully capable of doing to advance your career, and putting your dreams on hold for the sake of believing in us.

> Cobb: You're waiting for a train. A train that'll take you far away. You know where you hope this train will take you. But you can't know for sure. Yet it doesn't matter. Now, tell me why?
>
> Mal: Because you'll be together!
>
> *Inception*[1]

You either die a hero, or you live long enough to see yourself become a villain.

-Booker Dewitt, *Bioshock Infinite*[2]

[1] Nolan, C. *Inception.* (Warner Bros., 2010).
[2] *Bioshock Infinite*. (Irrational Games, 2013).

Table of Contents

List of Abbreviations vi
List of Figures vii
Acknowledgements viii
Abstract ix
Chapter 1 - Introduction 1
1.1 Viral hepatitis: disease, prevalence, treatment, and impact 1
1.2 Hepatitis C virus: history, transmission, genome, and replication cycle 2
1.3 HCV and oxidative stress: evidence and mechanisms 5
1.4 HCV induces DNA damage by increasing inflammation and oxidative stress 8
1.5 Project significance 10
Chapter 2 - Methods 12
2.1 Cell culture, collection, and drug treatments 12
2.2 Transient and stable transfections 12
2.3 Western Blotting 13
2.4 Immunofluorescence 13
2.5 Antibodies 14
2.6 Nox activity and hydrogen peroxide assays 14
2.7 Subcellular fractionation 15
2.8 Quantitative Reverse Transcriptase PCR 16
2.9 Statistical Methods 16
Chapter 3 - Results/Data Analysis 17
3.1 Transient expression of HCV core upregulates Nox levels in hepatocytes 19
3.2 Stable expression of HCV core upregulates Nox levels in hepatocytes 19
3.3 HCV core and Nox4 can localize to the nucleus and/or perinuclear space 20
3.4 HCV core elevates DNA damage markers through Nox protein 21
Chapter 4 - Discussion and conclusion 23
Chapter 5 - References 32
Chapter 6 - Figures 45

List of Abbreviations

Hepatitis C virus (HCV), chronic hepatitis C (CHC), hepatocellular carcinoma (HCC), National Notifiable Diseases Surveillance System (NNDSS), pegylated interferon (peg-IFN), direct acting antiviral (DDA), non-structural (NS), RNA-dependent RNA polymerase (RdRp), sustained virological response (SVR), hepatitis B virus (HBV), non-A, non-B hepatitis (NANBH), human immunodeficiency virus (HIV), untranslated region (UTR), internal ribosomal entry site (IRES), F protein/alternative reading frame protein (F/ARFP), envelope glycoprotein (E), interferon regulatory factor-3 (IRF-3), endoplasmic reticulum (ER), low density lipoprotein receptor (LDLR), glycosaminoglycan (GAG), heparan sulfate proteoglycan (HSPG), cluster of differentiation 81 (CD81), scavenger receptor B type 1 (SRB1), claudin (CLN1), occludin (OCLN), eukaryotic initiation factor (EIF), methionine initiator tRNA (Met-tRNAi), signal peptidases (SP), cytoplasmic lipid droplets (cLD), cytosolic phospholipase A2 (cPLA2), very low-density lipoproteins (VLDL), endosomal sorting complex required for transport (ESCRT), reactive oxygen species (ROS), phagocytic respiratory burst (PRB), glutathione peroxidase (GSH-Px), superoxide dismutase (SOD), glutathione (GSH), glutathione disulfide (GSSG), ferrous iron (Fe^{2+}), hydrogen peroxide (H_2O_2), ferric iron (Fe^{3+}), hydroxyl radical ($HO^{\cdot}$), polyunsaturated fatty acid (PUFA), 4-hydroxy-2-nonenal (HNE), malondialdehyde (MDA), electron transport chain (ETC), diphenyleneiodonium (DPI), cytochrome P450 2E1 (CYP2E1), inducible nitric oxide synthase (iNOS, or NOS2), tumor necrosis factor α (TNF-α), transforming growth factor β (TGF-β), interleukin-1β (IL-1β), interferon γ (IFN-γ), lipopolysaccharide (LPS), nitric oxide (NO^{-}), NADPH oxidase (Nox), superoxide anion ($O_{2}^{\cdot-}$), chronic granulomatous disease (CGD), natural killer (NK), copper-and-zinc SOD (Cu-Zn-SOD or SOD1/3), manganese SOD (Mn-SOD or SOD2), hepatic stellate cell (HSC), nuclear factor κB (NF-κB), non-like receptor protein 3 (NLRP3), single stranded breaks (SSB), double stranded breaks (DSB), 8-hydroxydeoxyguanosine (8-OHdG), 2'-deoxyguanosine (dG), 8-oxo-7,8-dihydro-2'–deoxyguanosine (8-oxodG), base excision repair (BER), nucleotide excision repair (NER), homologous recombination (HR), non-homologous end joining (NHEJ), apurinic/apyrimidinic (AP), AP endonuclease 1 (APE1), proliferating cell nuclear antigen (PCNA), flap endonuclease 1 (FEN1), transcription factor II H (TFIIH), single stranded DNA (ssDNA), breast cancer type 1, and 2 susceptibility (BRCA1/2), ataxia-telangiectasia mutated (ATM), H2A histone family, member X (H2AX), Japanese fulminant hepatitis 1 (JFH-1), human hepatocyte (Huh-7), Dulbecco's modified eagles medium (DMEM), phenylmethanesulfonyl fluoride (PMSF), immunofluorescence (IF), intracellular-like buffer (ICLB), ethylene glycol tetraacetic acid (EGTA), bicinchoninic acid (BCA), homovanillic acid (HVA), Hank's balanced salt solution (HBSS), horseradish peroxidase (HRP), ethylenediaminetetraacetic acid (EDTA), quantitative reverse transcriptase PCR (qRT-PCR), glyceraldehyde 3-phosphate dehydrogenase (GAPDH), analysis of variance (ANOVA), standard error of the mean (SEM), Centers for Disease Control (CDC), human hepatoblastoma (HepG2), phosphorylated H2A.X (H2A.X-γ), hypoxia inducible factor 1α (HIF-1α), dihydroethidium (DHE), secreted alkaline phosphatase (SEAP), vascular smooth muscle cells (VSMCs), nuclear localization signal (NLS), proliferator-activated receptor α (PPARα), TNF receptor 1 (TNFR1), phosphatase and tensin homologue (PTEN), IκB kinase (IKK), small interfering RNA (siRNA)

List of Figures

1. **Figure 1.** Nox expression with transient transfection of HCV core.
2. **Figure 2.** Nox activity and hydrogen peroxide production in hepatocytes transiently expressing HCV core.
3. **Figure 3.** Nox protein, mRNA, and enzyme activity levels and H_2O_2 production in hepatocytes stably expressing HCV core.
4. **Figure 4.** Immunofluorescence detection of core and Nox4 proteins in stable hepatocytes stably expressing HCV core.
5. **Figure 5.** Characterization of subcellular fractions and whole cell lysates from stable hepatocytes expressing core.
6. **Figure 6.** DNA damage markers in stable hepatocytes expressing core.
7. **Figure 7.** Nox activity is diminished in lysed hepatocytes treated with the novel Nox inhibitor, VAS-2870.

Acknowledgements

I would like to acknowledge Dr. David J. Lambeth for his gift of the Nox1 antibody, and Dr. Jing-hsiung Ou for his gift of the PCMV-RC plasmid used in this study. In addition, I would like to thank Dr. Masashi Kitazawa for his gift of the Alexa Fluor® 555 conjugated secondary antibody used for immunofluorescence.

This work was supported by NIH Grant R01CA158271 to Dr. Jinah Choi.

I would like to thank Drs. David Ojcius and Néstor Oviedo for serving on my thesis committee and providing me with guidance throughout my graduate studies. Furthermore, I would like to give thanks to lab members who provided assistance with experiments: Dr. Yiyan Wang, Jose Andres Vega, Macayla Kinney, David Fahim, Cameron Carlisle, and Qasim Javed.

Lastly, and most importantly, I would like to thank Dr. Jinah Choi for her knowledge, care, and ongoing support of me in spite of all who muddied the water to make it seem deep. I sincerely thank you!

Abstract

Role of hepatocyte NADPH Oxidase 4 in oxidative stress
and DNA damage by genotype 1a hepatitis C virus

Nicole Leanne Bidaud Corder
Master of Science

University of California, Merced
Dr. Jinah Choi

Hepatitis C virus (HCV) infection can lead to chronic infection resulting in severe liver diseases, including cirrhosis and hepatocellular carcinoma (HCC). Chronic hepatitis C (CHC) is characterized by ongoing inflammation and generation of reactive oxygen species (ROS) such as superoxide ($O_2^{\cdot -}$) and hydrogen peroxide (H_2O_2). NADPH oxidase (Nox) enzymes produce ROS as their primary function and have been associated with oxidative stress in CHC. However, the precise role that Nox enzymes play in the pathogenesis of HCC is still unclear. We show that the structural core protein of genotype 1a HCV is sufficient to elevate Nox1 and 4 mRNA, protein expression, and enzyme activity and H_2O_2 levels *in vitro*. Human hepatocytes constitutively expressing core exhibited elevated Nox4 in the nucleus and increased DNA damage markers. Furthermore, the novel Nox-specific inhibitor VAS-2870 was capable of decreasing the core-associated increase in Nox enzyme activity. Altogether, these results highlight the importance of developing therapeutic agents targeting Nox enzymes for use as adjunct treatment of CHC to prevent carcinogenesis.

Chapter 1 - Introduction

1.1 Viral hepatitis: disease, prevalence, treatment, and impact

Hepatitis C virus (HCV) is a major etiologic agent of severe and progressive liver disease that results in extensive liver injury, predisposing individuals to development of cancer.[1] Infection with HCV induces hepatic inflammation that can be characterized by two phases: acute and chronic infection. Acute hepatitis, the initial phase of the illness, lasts up to 6 months after primary viral exposure, and is characterized by a mild and often asymptomatic illness. Symptoms of acute infection, typically present in 20–30% of patients, are non-specific and can include mild fever, fatigue, muscle aches, loss of appetite, nausea/vomiting, joint pain, dark urine, or jaundice. Chronic hepatitis C (CHC) involves all intra- and extra-hepatic manifestations occurring after the acute phase of the infection.[2] Similar to the symptoms of acute illness, chronic hepatitis often presents as an asymptomatic illness. However, underlying liver injury is common and occurs in a progressive manner. The typical cascade of progressive liver damage begins with chronic inflammation of the liver, leading to fibrosis and the development of cirrhosis, followed by development of hepatocellular carcinoma (HCC). About 20–30 % of CHC patients develop cirrhosis within 20–30 years, and 4–7% of these individuals progress to HCC and end stage liver disease each year.[3]

In the United States, up to 85%, or an estimated 3.2 million HCV-infected persons suffer from chronic hepatitis C. Disease prevalence in the U.S. represents only a small proportion of the current global prevalence, estimated to be 174 million individuals, or 3.2% of the world population.[2,4,5] Regions with the highest prevalence (>3.5%) include Central and East Asia, North Africa, and the Middle East. Furthermore, it is estimated that between 3 and 4 million new cases of HCV arise every year.[6,7] In 2011, the number of acute HCV infections reported to the CDC totaled 1,229, an increase of 44% over the previous year. This elevation correlated with an increase in prevalence from 0.3 cases per 100,000 in 2010 to 0.4 cases per 100,000 in 2011 in the U.S. A total of 185,979 cases of CHC were reported to the National Notifiable Diseases Surveillance System (NNDSS) by 34 states in 2011. Furthermore, among viral hepatitis A, B, and C, hepatitis C accounted for the highest proportion of deaths in 2011, and an increase in mortality rate was observed from 4.4 deaths per 100,000 in 2006 to 4.7 deaths per 100,000 in 2010 in the U.S. In addition to the recent statistics indicating an increase in HCV prevalence, it is still estimated that approximately 50% of CHC infections remain undiagnosed and unreported in the U.S.[8]

Until recently, standard of care for treatment of HCV infection consisted of ribavirin and pegylated interferon (peg-IFN) administration, for which drug tolerance and treatment adherence is characteristically poor.[9] Development of direct acting antiviral (DAA) therapies within the last decade offers an alternative to the standard of care and

have greatly enhanced treatment outcomes in CHC patients. Common viral targets of DAAs include non-structural (NS) 3/4A protease, NS5A, and HCV RNA-dependent RNA polymerase (RdRp). For example, 61% of treatment-naïve subjects who were administered telaprevir, a protease inhibitor, for 12 weeks and peg-IFN/ribavirin regiment for 48 weeks achieved sustained virological response (SVR), compared to 41% treated with 12 weeks of placebo and 48 weeks of peg-IFN/ribavirin.[10] SVR, indicative of treatment success, is defined as having an undetectable HCV RNA level 24 weeks after the end of treatment. Furthermore, a nucleotide polymerase inhibitor, sofosbuvir, was recently approved by the FDA for use in conjunction with IFN, and as an IFN-free treatment option.[11] A clinical phase III trial in which treatment naïve participants with genotype 2 or 3 HCV were administered sofosbuvir and ribavirin for 12 weeks (n=256), or 24 weeks of peg-IFN and ribavirin treatment (n=243), 67% of participants from both groups achieved SVR at 12 weeks after discontinuation of therapy.[12] Once-daily oral daclatasvir, an inhibitor of NS5A, and sofosbuvir was associated with high rates of SVR among patients infected with HCV genotype 1, 2, or 3.[13]

Although significant advances have improved the overall survival and quality of life for patients with CHC, the incidence of HCC continues to rise.[14] In contrast to hepatitis B virus (HBV), there is no vaccine to prevent HCV infection and following development of chronic infection, disease progression occurs slowly over several decades. Physiological events that lead to the various disease states associated with HCV infection are complex. Reports indicate that from 2000 to 2005, the incidence rates of HCC were significantly higher in Hispanic, black, and white middle-aged men in which 1 year survival rates remained below 50% in the United States.[15] Given that many HCV-infected individuals experience only mild flu-like symptoms, or are asymptomatic, they are unaware of their HCV status.[3,16] Furthermore, by the time they are diagnosed, many patients have already progressed to an advanced disease state, which can complicate subsequent treatment.

1.2 Hepatitis C virus: history, transmission, genome, and replication cycle

HCV was originally isolated from the serum of a patient with non-A, non-B hepatitis (NANBH). The infectious agent was successfully cloned in 1989 and subsequently found to be responsible for 90% of post-transfusion NANBH in the United States.[17,18] Since its discovery, HCV remains a leading cause of chronic liver disease worldwide.[3] HCV, a blood borne pathogen, is transmitted from person to person via contact with contaminated blood or blood products. Identifiable risk factors implicated in the spread of HCV include receipt of contaminated tissues, organs, blood and/or blood products. In fact, before implementation of routine screening of donor blood in the early 1990's, receipt of contaminated blood products during blood transfusions and/or organ transplantation served as a significant source of infection. Another common risk factor is exposure to the virus through shared and repeated needle sticks/punctures during injection

drug use or body modification. The last risk factor involves close contact that is primarily sexual, but can include non-sexual contact, with individuals who have hepatitis C or are at risk of contracting the virus. Several subpopulations that have been identified as "at risk" groups include current or former injection drug users, individuals receiving ongoing hemodialysis or receipt of blood transfusions/organ transplants before July of 1992 or clotting factors before 1987. In addition, those with previous HBV or human immunodeficiency virus (HIV) infection, children born to HCV-positive mothers, and persons with known exposures, such as health care workers and blood or organ recipients from which the donor later tested positive are also at risk.

HCV is a single-stranded, positive sense RNA virus from the genus Hepacivirus of the family *Flaviviridae*. The viral genome is monopartite with a length of 9.6kb that contains coding and non-coding sequences. The non-coding sequences, or untranslated regions (UTR), flank either side of the coding sequence. The 5' UTR forms secondary structures that include an internal ribosomal entry site (IRES) essential for cap-independent translation of viral RNA. The coding sequence encodes for both structural and non-structural proteins. Structural regions include core, which encodes for the viral nucleocapsid protein and can code for F protein/Alternative Reading Frame Protein (F/ARFP), and envelope glycoproteins 1 and 2 (E1 and E2). Core protein will be discussed further below.

Nonstructural regions include, in order of appearance, NS1, NS2, NS3, NS4A, NS4B, NS5A, and NS5B. NS1 protein, or p7, is an integral membrane protein that belongs to the viroporin family exhibiting calcium ion channel activity, and was shown to be essential for viral infectivity in the chimpanzee model.[19–21] NS2, or p23, a transmembrane protein responsible for endoplasmic reticulum (ER) membrane association has been shown to exhibit protease activity facilitating cleavage of the NS2/3 region of the HCV polyprotein sequence.[22–24] NS3, or p70, is a multifunctional protein that exhibits serine protease activity when coupled with the NS4A cofactor, or p8, yielding the NS3/4A protease.[25] In addition, NS3/4A protease activity has been implicated in suppression of the host immune response by blocking activation of the antiviral signaling molecule, IRF-3.[26] NS4B, or p27, acts as an anchor for the viral replication complex and induces formation of the membranous web through rearrangement of the ER.[27–29] NS5A, or P56/58 can exist in two phosphorylation states, hypo- or hyper-phosphorylated.[30] NS5A induces formation of replication complexes necessary for genome replication and can also serve as a zinc metalloprotein.[31–33] Lastly, NS5B, or p68, an RNA-dependent RNA polymerase is essential to viral genome replication.[34,35]

Viral replication follows a series of sequential steps, beginning with attachment and receptor mediated endocytosis. Subsequent release of viral RNA, genome replication and translation occur in membranous webs associated with the ER. Lastly, viral assembly and release occur via budding through the plasma membrane. The process of HCV replication

has been described at length elsewhere.[36–39] Briefly, hepatitis C virus enters host cells through a complex set of interactions with various cellular membrane proteins. Initial attachment of free virions to hepatocytes occurs by way of association with three cell surface receptors; low density lipoprotein receptor (LDLR), glycosaminoglycan (GAG), and heparan sulfate proteoglycan (HSPG). Entry of viral particles occurs through clathirin-mediated endocytosis and requires interaction with the cell surface molecules, cluster of differentiation 81 (CD81), scavenger receptor B type 1 (SRB1), claudin (CLN1), and occludin (OCLN).[40] After endocytosis, vesicle acidification uncoats and releases the viral RNA into the cytoplasm.

Viral RNA is translated by host cell machinery and is initiated in a cap-independent and an IRES-dependent manner. In addition to the IRES, several viral proteins are involved in the translation of viral RNA, a process occurring in vesicular structures derived from the ER, known as membranous webs.[41] Briefly, the 40S ribosomal subunit associates directly with the IRES site forming a complex near the start codon.[42] Next, a 48S-like ribosomal initiation complex is formed by the adjoining eukaryotic initiation factors (eIF) 3 and eIF2, and a methionine initiator tRNA (Met-tRNAi) along with its associated GTP.[43] The structural conformation of the IRES and the 48S-like complex allows dissociation of phosphorylated eIF2 once translation is initiated.[44]

Translation occurs in the canonical 5’ to 3’ direction and produces a single polyprotein sequence approximately 3,000 amino acids in length that are processed by host and viral proteases co- and post-translation. Nine clearly defined proteolytic cleavage sites are located within the polyprotein sequence, generating at least ten non-overlapping proteins. Structural proteins are cleaved by cellular signal peptidases (SP), whereas non-structural proteins are cleaved by the viral proteases NS2/3 and NS3/4A. Upon cleavage of the various viral proteins, replication of viral RNA occurs via generation of a negative-sense RNA intermediate that serves as a template for mass production of positive-sense genomic RNA by viral RdRp. Positive-sense RNA generated *de novo* may be translated into viral proteins or encapsidated by core protein during virion assembly.

The comprehensive roles of the individual viral proteins encoded for by the HCV genome are still under investigation, but the process of assembly and packaging of new virions is facilitated by several key events. First, envelope glycoproteins 1 and 2 are trafficked to the lumen of the ER where they assemble into heterodimers. Next, core protein associates with cytoplasmic lipid droplets (cLD) under the assistance of cytosolic phospholipase A2 (cPLA2). Then, interactions between the ER transmembrane NS1 protein, cytosolic NS2, and NS3/4A facilitate the recruitment of core in the cytoplasm. During this process, viral RNA generated in the membranous web associates with core protein, whereby they migrate across the cytoplasmic space and bud into the lumen of the ER. The action of budding into the ER lumen is, in part, mediated by the interaction between core protein and envelope glycoproteins.

The process of viral maturation and release follows the secretory pathway of very low-density lipoproteins (VLDL), believed to occur through a series of budding and fission events involving the endosomal sorting complex required for transport (ESCRT).[25] Post-translational modification of E1 and E2 occur as virions transport through the Golgi apparatus where the proteins are prepared for post-release pH-dependent uncoating of virions in newly infected cells. Evidence shows viral NS1 acts as an ion channel stabilizing vesicle pH during maturation.[20,45–47] Finally, virions bud out through the plasma membrane.

1.3 HCV and oxidative stress: evidence and mechanisms

Oxidative stress is defined as a state of imbalance between the production and dismutation of reactive oxygen species (ROS) by cellular mechanisms that can disrupt cellular functions or induce cell damage. An important distinction should be made between the beneficial and detrimental effects of ROS. Specifically, though ROS are frequently associated with toxicity, their production is essential in the immunological destruction of microbes within phagosomes during the phagocytic respiratory burst (PRB).[48] In addition, ROS can regulate a variety of cellular processes through redox signaling.[49,50] Where the distinction between benefit and harm lies, is in the cumulative effect of ROS production occurring beyond the cell's ability to offset their toxic effects.

As the liver is the body's primary detoxifying organ, continued and chronic elevation of ROS can alter the body's antioxidant defenses. The antioxidant defense system is comprised of enzymatic components such as glutathione peroxidase (GSH-Px), superoxide dismutase (SOD), and catalase, in addition to non-enzymatic components including glutathione (GSH), and vitamins C and E. The enzymatic functions of GSH-Px, SOD, and catalase serve as a first line of defense against oxidative stress by facilitating the conversion of superoxide and hydrogen peroxide to less toxic species.[51]

Disrupted antioxidant defenses observed with CHC include decreases in glutathione (GSH) and vitamins C and E.[52] GSH is the most abundant non-protein endogenous thiol participating in redox homeostasis. GSH acts as a reducing agent in the detoxification of ROOH, a reaction catalyzed by GSH-Px that results in the formation of oxidized glutathione disulfide (GSSG). GSH also prevents membrane lipid peroxidation by maintaining the active forms of vitamin C and E in the cell.[53–55] Furthermore, antioxidant supplementation was shown to attenuate oxidative stress in CHC.[56] Structural proteins of HCV, specifically core protein, was shown to decrease reduced GSH and increase GSSG levels in hepatocytes *in vitro*. Conversely, hepatocytes expressing non-structural proteins increased GSH levels.[57] In addition, CHC patients showed higher GSH-Px levels post-treatment with interferon α-2b and ribavirin compared to baseline values.[58]

In addition to its role as the body's detoxifying organ, the liver also serves as a primary reservoir of iron. In hepatocytes and macrophages, approximately 20–30% of the

iron present remains bound to ferritin and hemosiderin.[59] Iron overload has been observed with CHC, and increased serum ferritin and iron levels were positively associated with HCV infection in the United States.[60] CHC is also associated with decreased expression of hepcidin, a negative regulator of iron expression, and upregulation of the hepatic iron transporter, transferrin receptor 2.[60–62] The role of iron in both the induction and propagation of oxidative stress is due, in part, to its oxidation and reduction properties. Ferrous iron (Fe^{2+}) can become oxidized by hydrogen peroxide (H_2O_2), producing the ferric form (Fe^{3+}) and hydroxyl radical ($HO^{\cdot}$) in a reaction known as the Fenton reaction.

Hydroxyl radical is a highly reactive species that causes damage to lipids, proteins, and DNA. Hydroxyl radical is known to interact with polyunsaturated fatty acids (PUFA), initiating lipid peroxidation in the cell that result in the formation of reactive products such as 4-hydroxy-2-nonenal (HNE) and malondialdehyde (MDA). Increased concentrations of lipid peroxidation products, and decreased GSH resulting from oxidative stress, were associated with steatosis and insulin resistance in CHC patients.[63,64]

Hepatocyte-specific sources originate primarily from enzymes in the mitochondria and the ER. A major source of mitochondrial ROS production is complex I of the electron transport chain (ETC).[65,66] Both genomic and subgenomic replicons containing core protein, as well as infectious HCV, were shown to increase mitochondrial ROS production. This elevation was completely abolished upon treatment with the flavoprotein inhibitor diphenyleneiodonium (DPI), suggesting that inhibition of complex I activity in the ETC may serve as an important source of mitochondrial ROS.[67–70] In addition, core protein was shown to associate with the outer mitochondrial membrane, leading to increased Ca^{2+} uptake and oxidation of glutathione pools, both of which enhanced susceptibility to mitochondrial depolarization.[70–73]

Cytochrome P450 2E1 (CYP2E1), found primarily in the ER of hepatocytes, is an important metabolizer of various small toxicological chemicals, including ethanol.[74] It is of note that CHC and ethanol consumption independently and cumulatively increase oxidative stress in the liver.[75] One study showed elevation of CYP2E1 in the livers of five CHC patients exhibiting early fibrosis, and *in vitro* studies showed co-expression of CYP2E1 and HCV core protein was associated with increased ROS production.[76–78] Another enzyme of the ER that contributes to imbalances in redox homeostasis is inducible nitric oxide synthases (iNOS, or NOS2). Up-regulation of iNOS in hepatocytes, Kupffer cells, and macrophages occur in response to various pro-inflammatory cytokines, including tumor necrosis factor α (TNF-α), transforming growth factor β (TGF-β), interleukin-1β (IL-1β), interferon γ (IFN-γ) and/or lipopolysaccharide (LPS).[79] iNOS catalyzes the formation of nitric oxide (NO^{-}) from NADPH and L-citrulline, and it's upregulation has been associated with HCV in cell culture systems.[80–83]

Additional sources of oxidative stress in hepatocytes, and non-hepatocytes, are NADPH oxidase (Nox) enzymes. Nox enzymes perform diverse physiological roles,

ranging from thyroid hormone synthesis, maintenance of equilibrioception, signaling in the vascular system, and antimicrobial processes of the immune system. The Nox family consists of seven transmembrane proteins, Nox and Dual oxidase (Nox1 through 5 and Duox 1 and 2) whose primary function is to catalyze the transfer of electrons from NADPH to O_2 to generate superoxide and H_2O_2.[84] Among these proteins, the role of Nox2 in the immune response has been widely characterized.

Nox2, also referred to as $gp91^{phox}$ or simply phox (phagocytic oxidase), functions in the PRB. When activated in response to pathogens, transmembrane Nox2 coupled with its catalytic subunit $p22^{phox}$, associate with various activating cytosolic factors, $p67^{phox}$, $p40^{phox}$, $p47^{phox}$, and Rac. Upon their association, large quantities of oxygen are reduced to generate superoxide anion ($O_2^{\cdot-}$) that effectively destroys phagocytized pathogens. The importance of Nox2 in this process is easily observable in patients with chronic granulomatous disease (CGD), where mutations in one or more of the catalytic subunits of Nox2 or its cytosolic factors, produce an insufficient respiratory burst that results in aberrant inflammation and increased susceptibility to infections.[85]

Several sources show activation of Nox2 in phagocytes and monocytes with HCV infection. Specifically, NS3 protease was shown to activate phagocytic Nox2 leading to apoptosis in T cells, natural killer (NK) cells, and cytotoxic T cells.[86,87] In addition, extracellular secreted core protein of HCV was capable of inducing signal transducer and activator of transcription 3 (STAT3) in an IL-6 autocrine-dependent manner. As STAT3 is an activator of the $p47^{phox}$ cytosolic factor of Nox2, and authors report induction of myeloid-derived suppressor cells by HCV core protein, this suggests suppression of T cells may occur in an ROS-dependent manner.[88,89]

Other Nox isoforms expressed in hepatocytes include Nox1 and 4, transmembrane proteins of the Nox family that remain bound to their $p22^{phox}$ catalytic subunit. Similar to Nox2, Nox1 produces ROS when activated by the association of the cytosolic subunits NoxO1, NoxA1, and Rac. Like other Nox enzymes, Nox4 is composed of six predicted transmembrane domains and an intracellular carboxyl-terminal region containing FAD and NADPH binding sites.[90] Truncated Nox4 proteins lacking the C-terminal FAD and NADPH binding sites are unable to transport electrons and show negative effects on the endogenous Nox4 activity.[91] Furthermore, the Nox4 intracellular B loop, located between transmembrane domains 2 and 3, is essential for its enzyme activity, and the intracellular D loop is necessary for the structural interaction between Nox4 and the $p22^{phox}$ subunit. To date, five alternatively spliced isoforms of Nox4 have been reported.[92] Compared to full length Nox4 (~67kDa), variant B (~63kDa) lacks the first NADPH binding site, while variant C (26kDa) does not contain any FAD or NADPH binding sites due to a frameshift-derived stop codon after transmembrane domain 5. Variant D (32kDa) contains transmembrane domain 1 and all FAD and NADPH binding sites, while variant E (28kDa) is similar to variant D, except for absence of the first NADPH binding domain.[92]

Nox4 was shown to contribute significantly to nuclear superoxide production in hepatocytes.[93,94] Recently, Anilkumar *et al*. observed a functional 28kDa splice variant of Nox4 within the nucleus and nucleolus of vascular cells that was able to generate ROS in an NADPH-dependent manner.[95] Furthermore, HCV has been shown to elevate superoxide and hydrogen peroxide production via an up-regulation of Nox1 and Nox4 protein expression in hepatocytes in addition to nuclear and/or perinuclear localization.[93] Dominant negative Nox4, and Nox4 knockdown, significantly decreased HCV-associated ROS production in hepatocytes.[93,96] Additionally, increases in $p22^{phox}$, $p67^{phox}$, NOXA1, and NOXA2 mRNAs were also observed.[93] Furthermore, Nox4 and Nox1 protein levels as well as Nox activity were elevated in human livers infected with HCV.[85] Nox4 elevation by HCV and transcriptional activation of Nox4 promoter activity by core protein were shown to be mediated by TGF-β.[96]

1.4 HCV induces DNA damage by increasing inflammation and oxidative stress

Chronic inflammation of the liver occurs in response to HCV infection. Inflammatory cells of the liver such as Kupffer cells and neutrophils generate ROS to combat viral infection. However, a prolonged state of inflammation may render HCV-infected and naïve hepatocytes susceptible to ROS generated by immune cells. In particular, hydrogen peroxide is freely diffusible across plasma membranes and the extracellular space.[97] Furthermore, superoxide generated in the intracellular space is readily converted to hydrogen peroxide and molecular oxygen by SOD enzymes; copper-and-zinc SOD (Cu-Zn-SOD, or SOD1/3) are present in the cytoplasm of all eukaryotic cells, and manganese SOD (Mn-SOD, or SOD2) dismutate superoxide generated in the mitochondria.

Long-term maintenance of inflammation in CHC occurs in response to activation of inflammatory cytokines such as TNF- α, TGF-β, and IL-1β. These cytokines are elevated with HCV infection, and have been shown to play a pivotal role in the development of CHC. TNF-α induces oxidative stress through the mitochondrial ETC and may play a role in the proliferation of hepatocytes characteristic of fibrosis and HCC.[98] However, the primary inducer of liver fibrosis via a redox-sensitive mechanism is through elevated TGF-β. Induction of TGF-β in hepatocytes and hepatic stellate cells (HSC) was shown to occur in a nuclear factor κB (NF-κB) –dependent manner. Specifically, one study showed core protein was able to directly upregulate TGF-β reporter activity and expression in hepatoma cells.[99] In addition, activation and maturation of IL-1β is facilitated by inflammasome formation and cellular nod-like receptor protein 3 (NLRP3) expression, both of which were elevated in Kupffer and hepatoma cells.[100,101]

Aside from the cyclic roles that inflammation and oxidative stress play in the maintenance of one another, consequential DNA damage is cumulative and capable of initiating carcinogenesis, a hallmark of CHC disease progression.[102,103] This is particularly

true when lesions occur in tumor suppressor genes and proto-oncogenes. Potential to damage DNA exists with most ROS, particularly when generated in close proximity to the nucleus. DNA damage is characterized by lesions in bases and/or the deoxyribosyl backbone, and can include deaminated bases, abasic sites, formation of bulky adducts, single stranded breaks (SSB), and double stranded breaks (DSB). One specific redox mediated product of DNA damage that has been implicated in HCC is 8-hydroxydeoxyguanosine (8-OHdG), which is formed by interaction of 2'-deoxyguanosine (dG) with reactive species such as $HO^{\cdot}$, $O_2^{\cdot-}$, and peroxynitrite ($ONOO^-$).[104] Once formed, 8-OHdG can induce G:C to T:A transversions that are frequently observed in cancer. Levels of 8-OHdG have been positively correlated with HCC grade in CHC versus non-CHC patients, and in HCV versus HBV.[105–108] Furthermore, association of 8-OHdG with DSBs has been shown to occur by Fenton chemistry.[109] Another product that augments DNA damage with HCV is $ONOO^{\cdot}$, produced by reaction between $O_2^{\cdot-}$ and $NO^{\cdot}$. $ONOO^-$ generated in the nucleus is capable of attacking bases and the deoxyribosyl backbone of DNA, where it forms 8-oxo-7,8-dihydro-2'-deoxyguanosine (8-oxodG), another biomarker of oxidative stress.[110,111]

In addition to causing DNA damage, HCV exhibits the ability to block repair mechanisms that aim to correct oxidative damage. Common mechanisms of DNA damage repair include base excision repair (BER), nucleotide excision repair (NER), homologous recombination (HR), and non-homologous end joining (NHEJ). BER removes small, non-helix-distorting lesions in the DNA such as those caused by deaminated, alkylated, or oxidized bases. Initiation of BER occurs when lesions are recognized and excised by DNA glycosylases, leaving either an SSB or an apurinic/apyrimidinic (AP) site. The enzyme AP endonuclease 1 (APE1) is essential in repair of ROS-mediated DNA damage. Indeed, HCV infection is associated with elevations in APE1 and 8-OHdG accumulation.[112] Functionally, APE1 is responsible for processing AP sites before initiating either short-patch BER or long-patch BER.[113] Short-patch BER inserts a single nucleotide via polymerase β and a complex containing DNA ligase III and XRCC1. In contrast, long-patch BER replaces between 2 and 12 nucleotides by proliferating cell nuclear antigen (PCNA), flap endonuclease 1 (FEN1), and one, or more, of several polymerases.

NER, in contrast to BER, removes bulky helix-distorting DNA adducts in one of two ways, through global genome NER, or transcription coupled NER. Both processes are initiated upon detection of bulky adducts by detector proteins that readily bind to oxidative lesions, namely XPC and XPE, or CSA and CSB in global genome NER and transcription coupled NER, respectively.[114] However, the frequency with which NER is employed over BER in repairing oxidative damage is unclear. Upon recognition of damage, proteins of the transcription factor II H (TFIIH) complex guide unwinding of the DNA helix and removal of the bulky adduct. Subsequent gap filling requires PCNA and one of various polymerases, and is followed by ligation. Ligation is carried out by XRCC1 and DNA ligase III.[115]

HR and NHEJ are two widely studied pathways that repair extensive DNA damage caused by DSBs. The processes of HR and NHEJ have been described at length elsewhere.[116] Between the two processes, NHEJ promotes direct ligation at the expense of introducing errors to the DNA in the form of insertions, deletions, substitutions, and translocations. In contrast, HR generates many single stranded DNA (ssDNA) overhangs that an assembled nucleoprotein filament capable of using homologous duplex DNA to produce crossover and non-crossover products.[117] The mechanisms that contribute to the cellular decision to repair DSBs by HR versus NHEJ are complex, but the efficiency of repair are likely influenced by the location of the damage and cell cycle stage.[118,119]

Both structural and non-structural proteins of HCV have been associated with alteration in DNA repair mechanisms. Structural core protein is capable of binding NBS1 and preventing formation of the MRN complex that requires adjoining of Mre11 and Rad50 to NBS1.[120] The MRN complex is involved in the initial processing events that proceed HR and NHEJ, and has been suggested to act as a regulator when deciding between the two DSB repair mechanisms.[116] Other proteins identified as potential decision makers with respect to undergoing HR are the breast cancer type 1, and 2 susceptibility (BRCA1/2) proteins. BRCA1 and BRCA2 are essential in the transcription-coupled repair of 8-OHdG lesions, a common occurrence with HCV infection.[121,122] Non-structural proteins NS3 and NS4A decreased expression of ataxia-telangiectasia mutated (ATM), a serine/threonine protein kinase that phosphorylates cell cycle checkpoint proteins activated in response to DSBs.[123] Downstream targets of ATM include p53, Chk2, and H2A histone family, member X (H2AX). Furthermore, core protein modulates p53, a tumor suppressor protein, by altering its DNA binding affinity, and interacting with its promoter region. These interactions lead to increased cell proliferation, independent of p53 expression, and suppression of apoptosis.[124–128] Additional targets of core protein, for which the effects lead to increased cell proliferation, include the cyclin-dependent kinase inhibitor p21 (WAF1), and proto-oncogenes *c-Myc* and *c-Jun*, to name a few.[127,129–132] Several other targets of core protein have been outlined elsewhere.[133]

1.5 Project significance

The study of HCV has been largely dictated by the availability of virus-producing cell culture systems and animal models that aim to mimic human infection. As the Japanese Fulminant Hepatitis 1 (JFH-1) strain of HCV was the first to support robust replication *in vitro*, it is reasonable that most work with HCV has been conducted using this genotype 2a system. However, it is of note that the severity of hepatitis C infection is correlated with genotype, as evidenced by the FDA's recent approval of genotype tests to aid clinicians in treating and ultimately managing HCV infection in patients. Of the 6 distinct genotypes of HCV, genotype 1 is the most prevalent in North America and Europe, accounting for approximately 70% of cases in the United States. Given the importance of genotype in

assessing treatment response, this indicates that treatment outcome, and the severity of disease progression are associated with HCV genotype. Indeed, infection with genotype 1 HCV is more highly associated with development of chronic infection and is characteristically harder to treat. For example, 80% of patients infected with HCV genotype 2 or 3 achieve SVR with standard IFN-based therapy, compared to 42–46% of those infected with genotype 1.[13]

The primary efforts in treating HCV-induced disease are focused on reducing, or eliminating the virus from patients to prevent transmission as well as chronic liver injury. However, with over 170 million people chronically infected with the virus, the effects of increased oxidative stress have already predisposed these individuals to liver cirrhosis, and eventual development of HCC. Therefore, treatment aimed at halting the pathogenic mechanisms of HCV infection would provide many individuals with relief and perhaps prevent disease progression. To date, no studies have clearly determined the role of Nox proteins and oxidative stress-associated DNA damage with genotype 1 HCV. Therefore, the aim of this study is to assess the role Nox proteins play in DNA damage associated with genotype 1 HCV in HCC, and elucidate their potential relevance to therapy. We hypothesize that core protein is sufficient to elevate Nox enzymes, particularly Nox4, which may induce nuclear localization that can cause DNA damage.

Chapter 2 - Methods

2.1 Cell culture, collection, and drug treatments

Human hepatocytes (Huh-7) were cultured and grown in Dulbecco's Modified Eagles Medium (DMEM), supplemented with 10% fetal bovine serum (FBS), and 1% Penicillin/Streptomycin, all purchased from Life Technologies. Cells were grown in 60mm dishes purchased from Corning, corresponding to a surface area of 2.872cm^2. Drug treatments were added to cell culture medium for 1 hour, unless otherwise noted. Diphenyleneiodonium chloride (Sigma Aldrich) was dissolved in water and administered at a final concentration of 10µM. VAS-2870 (Enzo Life Sciences) was dissolved in DMSO and administered at final concentrations ranging from 5–20µM. DMSO concentrations did not exceed 0.01% (vol/vol). All cell collections were performed by washing twice with 1x phosphate buffered saline (PBS) to remove residual media, followed by addition of an appropriate volume of 1x PBS with protease and phosphatase inhibitors; 10µM sodium fluoride, 1µM protease inhibitor cocktail, 1µM sodium orthovanadate, 1µM phenylmethanesulfonyl fluoride (PMSF). All chemicals used in this study were purchased from Sigma Aldrich, unless otherwise specified. Cells were then collected by scraping and were immediately placed on ice before processing. Cells were lysed in either 2x Laemmli buffer, or RIPA buffer with protease and phosphatase inhibitors, by sonication on ice 3 to 4 times for 15 second intervals. Lysates were centrifuged at top speed for 10 minutes at 4°C and then stored at -20°C until use.

2.2 Transient and stable transfections

Huh-7 cells were seeded and grown to 50–60% confluency before transfection. Transfections were conducted via calcium phosphate precipitation using ProFection® Mammalian Transfection System (Promega Corporation) with the following modifications to the manufacturer's protocol. DNA-calcium phosphate co-precipitation was achieved by pipette-driven aeration from the bottom of each microcentrifuge tube for 60 seconds. Microcentrifuge tubes were then left at room temperature for 20 minutes to facilitate generation of a fine precipitate before drop-wise addition to cell culture medium. Four hours after addition of the transfection mixture, cells were washed twice with 1x PBS before fresh media was added. For transient transfections, cells were collected 48 hours post-transfection with empty vector pRc-CMV (Life Technologies), or pCMV-RC plasmid (full genotype 1a HCV core coding sequence of the RH strain) generated as described elsewhere.[134] Stable cells were selected by daily treatment with 0.5mg/ml G418 sulfate (Gibco), as described previously.[93]

2.3 Western Blotting

Western blotting was performed with Novex® Tris-Glycine gels (Life Technologies) using the manufacturer's guidelines. Proteins were transferred to PVDF membranes (Immobilon-P from Millipore) overnight at 4°C with low voltage using Bio-Rad's Tetra Blotting Module. Membranes were washed 3 times with 1x Tris-buffered saline (TBS) for 10 minutes, and blocked with 5% (wt/vol.) non-fat dry milk (NFDM) in TBS for 1 hour at room temperature with gentle agitation. Primary antibodies were diluted in 5% NFDM in TBS supplemented with 0.1% (vol/vol) Tween-20 (TBS-T) before addition to membranes. Membranes were incubated with primary antibodies overnight at 4°C with gentle agitation. Before addition of secondary antibodies, membranes were again washed 3 times with TBS-T for 10 minutes at room temperature. Secondary antibodies, diluted in 5% NFDM/TBS-T, were incubated with membranes at room temperature with agitation for 1 hour. Membranes were washed 3 times with TBS before chemiluminescent detection with Amersham ECL Prime Western Blotting Detection Reagent (GE Healthcare Life Sciences). Membrane visualization with a Kodak Image Station detector was performed 3–5 minutes after exposure to chemiluminescent reagent as per manufacturer's protocol. Densitometry analyses were performed using Image Studio Lite (LI-COR Biosciences) and subsequent calculations included normalization to appropriate cellular protein intensities.

Blotting and detection of phosphorylated proteins was performed as follows. After transferring, PVDF membranes were washed 3 times with TBS, and blocked with 5% bovine serum albumin (BSA)/TBS-T for 1 hour at 4°C with gentle agitation. BSA was purchased from Santa Cruz Biotechnologies. Membranes were then washed an additional 3 times before overnight incubation at 4°C with phospho-specific primary antibodies diluted 1:1000 in 5% BSA/TBS-T. Membranes were then washed 3 times with TBS-T before a 1 hour incubation with secondary antibodies diluted 1:2000 in 5% BSA/TBS-T. Then, membranes were washed 3 more times before chemiluminescent detection described above.

2.4 Immunofluorescence

For immunofluorescence (IF) detection of proteins, cells were seeded and grown on glass coverslips for 24 hours in 35mm dishes (Corning). Cells were washed twice for 5 minutes with 1x PBS before fixation. Cell fixation was achieved with 10 minutes of 1:1 methanol-acetone treatment at -20°C. After fixation, cells were washed 3 times with 0.5% (wt/vol) BSA in 1x PBS (PBB) solution. Coverslips were blocked using 2% BSA in 1x PBS for 1 hour at room temperature. Primary antibodies, diluted in 1x PBB, were applied to coverslips and incubated overnight at 4°C in a moist environment. Coverslip were further washed before incubation with fluorophore-conjugated secondary antibodies (Santa Cruz Biotechnology, Inc.) diluted in PBB for 1 hour in the dark. Coverslips were then

washed with PBB and PBS before mounting on glass slides using Fluoromount-G (Southern Biotechnology Associates, Inc.) and visualization with a confocal microscope.

2.5 Antibodies

Primary antibody controls used for Western Blotting in this study were goat β-actin (I-20), goat calnexin (C-20), mouse HCV core (C7-50), goat PCNA (C-20), mouse LSD1 (B-9), goat fibrillarin (A-16) and rabbit NF-κB p65 (C-20), all of which were purchased from Santa Cruz Biotechnology, Inc. Three rabbit Nox4 antibodies were used in Western Blotting and IF, NB110-58849, ab133303, and ABC271, from Novus Biologicals, Abcam, and EMD Millipore, respectively. Rabbit HCV core (ab58713) from Abcam was used for IF detection of core protein, and mouse lamin A/C (N-18) from Santa Cruz Biotechnology was used as a nuclear control marker. Antibodies used to study the DNA damage response by Western Blotting were rabbit HIF-1α (bs-0737R) from Bioss Inc., rabbit phospho-Histone H2A.X (Ser139) (2577), and rabbit Histone H2A (2572) from Cell Signaling Technology.

Secondary antibodies used in Western Blotting were donkey anti-goat IgG-HRP (sc-2020), goat anti-rabbit IgG-HRP (sc-2004), and goat anti-mouse IgG-HRP (sc-2005) all from Santa Cruz Biotechnology. Fluorophore-conjugated secondary antibodies used in IF were goat anti-mouse IgG, $F(ab')_2$-TRITC (sc-3796) and goat anti-rabbit IgG, $F(ab')_2$-FITC (sc-3839) from Santa Cruz Biotechnology. In addition, goat anti-mouse IgG, $F(ab')_2$-Alexa Fluor® 555 (H+L) from Life Technologies, a kind gift of Dr. Masashi Kitazawa, was used.

2.6 Nox activity and hydrogen peroxide assays

Nox activity was measured by SOD-inhibitable cytochrome c reduction. Assays were performed on cells seeded in 6-well plates and grown to 80% confluency before experiments. For whole cell cytochrome c reduction detection, cells were washed once with cold PBS, then once with cold intracellular-like buffer (ICLB). In contrast, lysed cell Nox activity was measured after physically dislodging cells in ICLB with protease and phosphatase inhibitors, followed by 3 rounds of sonication for 15 seconds while incubating on ice. ICLB was prepared before experiments and contained 140mM potassium chloride, 1mM magnesium chloride, 10mM D-glucose, 10mM HEPES, 0.193mM calcium chloride dehydrate, and 1mM ethylene glycol tetraacetic acid (EGTA). The pH was adjusted to 7.40 with 2M potassium hydroxide, the solution was filter sterilized, and stored at 4°C before use.

Cells were permeabilized with 0.4mM digitonin solution, dissolved in ICLB, for 5 minutes at 35°C. Then, cells were washed 2 times with ICLB and incubated in pre-treatment solutions for 15 minutes at room temperature. Pre-treatment solutions were 10μM DPI dissolved in water, 200 units/ml SOD from bovine liver (dissolved in PBS),

and/or solvents as controls. Cytochrome c cocktail, prepared fresh before use, was added to each well with target concentrations of 80µM cytochrome c from equine heart, 100µM NADPH, 100µM ATP, and 100µM GTP. Cells were incubated with cytochrome c cocktail in a dry incubator with agitation for 60 minutes, unless otherwise specified. Supernatant solutions were collected and centrifuged briefly before plating in an optically clear 96-well plate. Absorbance at 550nm, with a reference at 540nm, was obtained using a SpectroMax M2 spectrophotometer (Molecular Devices). Measurements were normalized to total protein content measured by Pierce bicinchoninic acid **(**BCA) protein assay (Thermo Scientific) as indicated by the manufacturer's protocol.

Hydrogen peroxide production was measured by detection of the fluorescent dimerization of homovanillic acid (HVA). Cells were treated with 10µM DPI or solvent for 30 minutes in a 5% CO_2 incubator. HVA-peroxidase reaction buffer, containing 0.40mM HVA and 4.0 units/ml horseradish peroxidase (HRP) type II, dissolved in HBSS was prepared fresh before use. Reaction buffer was added to each well, followed by the treatment reagents at a final concentration of 10µM DPI, 200 units/ml, or solvent as a control. The cells were incubated in a 5% CO_2 incubator for 120 minutes, unless otherwise specified. The supernatant was collected and the reaction was stopped by the addition of 0.10M L-glycine, followed by plating in an optically clear 96-well plate. Fluorescence was then measured by excitation at 321nm and emission at 421nm, and the values were normalized by total protein content described above.

2.7 Subcellular fractionation

Cytoplasmic, nuclear, and post-nuclear extracts were obtained using the following protocol. Cells were seeded in 100mm dishes and grown to 80% confluency before fractionation. Cells were collected in 1x PBS with protease and phosphatase inhibitors, and then packed by centrifugation at top speed for 1 minute at 4°C. The cell pellet was suspended in an appropriate volume (dependent on pellet size) of hypotonic buffer with protease and phosphatase inhibitors. Hypotonic buffer contained 10mM HEPES (pH 7.90), 0.5% (vol/vol) IGEPAL, 2mM magnesium chloride, 10mM potassium chloride, and 0.1mM ethylenediaminetetraacetic acid (EDTA).

The cells were mixed by vortexing well and then incubated on ice for 10 minutes. The samples were then centrifuged at top speed for 2 minutes at 4°C to obtain the cytoplasmic fraction. The remaining pellet was suspended in high salt buffer, at one fourth of the volume of hypotonic buffer, with protease and phosphatase inhibitors. High salt buffer contained 50mM HEPES (pH 7.90), 300mM sodium chloride, 50mM potassium chloride, and 0.1mM EDTA. Then, the samples were vortexed for 1 minute every 10 minutes for a total of 1 hour. The nuclear extract was obtained from the resulting supernatant after 6 minutes of top speed centrifugation at 4°C. The leftover cell debris was

solubilized by sonication in 2x Laemmli buffer. BCA protein assay was performed on the cytoplasmic and nuclear fractions, followed by Western Blotting on all 3 fractions.

2.8 Quantitative Reverse Transcriptase PCR

Total intracellular RNA was extracted using TRIzol reagent (Life Technologies) as recommended by the manufacturer's protocol. Nox mRNA levels were quantified using real time quantitative reverse transcriptase PCR (qRT-PCR). The EXPRESS SYBR GreenER Universal kit (Life Technologies) was used, and cycle threshold (C_T) values were obtained using a 7500 RT-PCR system (Applied Biosystems). Nox1 and Nox4 mRNA levels were calculated using relative quantitation using the $\Delta\Delta C_T$ method with glyceraldehyde 3-phosphate dehydrogenase (GAPDH) as an internal control. Primer sequences were as follows. Nox1 primers were *CCTGAGTCTTGGAAGTGGATC* (forward), and ACGCTTGTTCATCTGCAATTC (reverse). Nox4 primers were TCACAGAAGGTTCCAAGCAG (forward), and ACTGAGAAGTTGAGGGCATTC (reverse). GAPDH primers were GGTGGTCTCCTCTGACTTCAA (forward), and GTTGCTGTAGCCAAATTCGTT (reverse). All primer sequences are written in the 5' to 3' direction.

2.9 Statistical Methods

Data were analyzed using student's t-test, or one way analysis of variance (ANOVA) with SigmaPlot version 13.0 (Systat Software, Inc.). A P value ≤ 0.05 was considered statistically significant, and data were calculated as average ± standard error of the mean (SEM).

Chapter 3 - Results/Data Analysis

HCV is a major contributor to severe and progressive liver diseases, including fibrosis, cirrhosis and HCC. Approximately 75–85% of those who become infected will develop CHC, defined as infection persisting greater than 6 months.[2] Of those who develop CHC, 20–30% will progress to cirrhosis within 2–3 decades, and 4–7% will develop HCC each year thereafter.[3] Furthermore, the Centers for Disease Control (CDC) reported a 44% increase in new cases of HCV infection in 2011 over the previous year. Despite heightened awareness and routine screening of donor blood and tissue products, most infected individuals are asymptomatic during the course of their illness, it is estimated that 50% of CHC cases remain undiagnosed and thus unreported in the United States.[8]

HCV is an enveloped, positive sense RNA virus of the family *Flaviviridae*. The monopartite genome is 9.6kb in length and consists of structural and nonstructural genes flanked by untranslated regions that aid in viral gene replication and expression. There are six distinct genotypes (1–6) and various subtypes ranging from a–h, where genotype 1 comprises the majority of infections in North America and Europe; up to 70% of infections in the U.S. are of genotype 1.[13] Translation of the HCV genome produces a single polyprotein that is cleaved by viral and cellular signal peptidases. Structural proteins include core, responsible for nucleocapsid formation, and envelope glycoproteins 1 and 2. NS proteins, responsible for viral replication, polyprotein processing and viral assembly and exit, consist of P7, NS2, NS3, NS4A/B, and NS5A/B. The functions of NS proteins have been reviewed elsewhere.[25,135]

A hallmark of CHC is increased oxidative stress, a consequence that is widely believed to serve as the primary mechanism by which the accumulation of liver damage predisposes carcinogenesis. Oxidative stress is defined as an imbalance between the cellular production and detoxification of ROS such as superoxide ($O_2^{\cdot -}$), H_2O_2, and $HO^{\cdot}$. A key feature of ROS, as the name implies, is their ability to react with cellular components and effectively perturb homeostasis. Oxidative damage to the liver that is consistent with CHC arises from both non-hepatocyte and hepatocyte sources. Non-hepatocytes such as monocytes and Kupffer cells produce and release superoxide during the phagocytic respiratory burst (PRB) in response to invading pathogens.[136] Superoxide can readily dismutate to H_2O_2 by the enzymatic action of superoxide dismutase (SOD). Then, H_2O_2 can be reduced to $HO^{\cdot}$ by ferrous iron (Fe^{2+}) in Fenton chemistry, converted to hypochlorous acid (HOCl) by myeloperoxidase (MPO) where it exerts a powerful toxic effect on invading microbes, or detoxified by glutathione (GSH) to water. However, despite the antimicrobial benefit of the PRB, the cytotoxicity induced by the production and release of ROS in the intra- and extracellular space of hepatic immune cells can overwhelm antioxidant defenses in hepatocytes, and thus contribute to oxidative stress.

Hepatocytes produce oxidative stress in response to HCV through a number of mechanisms. One mechanism considered to be the largest contributor to hepatocyte

oxidative stress occurs via inhibition of complex I in the electron transport chain of mitochondria by core protein, resulting in excessive production of $O_2^{-\cdot}$ and elevation of CYP2E1 and iNOS enzyme expression in the ER. In addition, the depletion of mitochondrial GSH pools in response to disruptions in calcium release from the ER has been attributed to the association of core protein with the outer mitochondrial membrane. The liver is the primary detoxifying organ in the body and serves as a significant reservoir of the body's iron remaining bound to hemosiderin and ferritin. Therefore, hepatocyte sources of oxidative stress exhibit a significant effect on other functions of the liver, leading to extra-hepatic manifestations.

Another mechanism by which hepatocytes produce ROS, is through increased expression of NADPH oxidase (Nox) enzymes. Nox4 has been identified in various subcellular compartments, including the plasma membrane, ER, and mitochondria.[137,138] In addition to full-length Nox4, four other splice variants have been identified and characterized in human lung (A549) cells.[92] Comparison of prototype Nox4 with its splice variants revealed structural differences largely characterized by the absence of one or more exons. For example, isoforms B and E lack one of several NADPH-binding domains. In addition, isoforms D and E lack all but one transmembrane domain, which may serve as an explanation for differences in subcellular location of Nox4. Recently, Anilkumar, *et al.* demonstrated, by immunofluorescence and Western Blotting, that a 28kDa splice variant corresponding to isoform D localizes to the nuclear and/or nucleolar space in human embryonic kidney (HEK) cells. Furthermore, they confirmed ROS production by nuclear Nox4D, measuring H_2O_2 production by homovanillic acid (HVA) assay, and $O_2^{-\cdot}$ production by lucigenin-enhanced chemiluminescence.[95]

Additionally, several authors have reported the effects of ROS generation on cell signaling, and oxidative stress-associated DNA damage. For example, overexpression of Nox4 was shown to disrupt phosphorylation events in the nucleus that increased phosphorylated extracellular signal-regulated kinase (ERK) 1/2, resulting in alterations in vascular smooth muscle cell (VSMC) signaling.[95] Furthermore, Boudreau *et al.* showed genotype 1a HCV increased Nox4 mRNA and protein expression, as well as superoxide generation in human hepatoblastoma (HepG2) cells.[96] In addition, core-dependent increases in Nox4 and oxidative stress were shown to occur through an autocrine-dependent up-regulation of the profibrogenic cytokine TGF-β1.[96,99]

Core-dependent inhibition of DNA damage repair has also been suggested. Keigo *et al.* showed genotype 1b core protein interacted with the DNA repair protein NBS1, preventing formation of the MRN complex and subsequent activation of ATM, necessary for repair of DSBs in the DNA.[120] In this study, we show that genotype 1a core is sufficient to increase oxidative stress by elevation of Nox1 and Nox4 at the mRNA and protein levels, in addition to increasing Nox enzyme activity and hydrogen peroxide production. Also, the oxidative stress induced by core protein elevated markers of DNA damage consistent with

breaks in the genome. Furthermore, treatment with the novel Nox-specific inhibitor VAS-2870 was capable of decreasing core-associated elevations in Nox activity.

3.1 Transient expression of HCV core upregulates Nox levels in hepatocytes

To test whether HCV core expression led to increased Nox levels in hepatocytes, Huh-7 cells were transiently transfected with 0–2µg of HCV core (1a) expressing plasmid under the CMV promoter, or control plasmid (pRc-CMV) and evaluated for Nox expression by Western Blotting. Core protein could be detected in all samples transfected with core expression construct, and the protein level was 1.55- and 2.65-fold higher in transfectants with 1.0µg and 2.0µg of core, respectively when compared to samples transfected with 0.5µg of core plasmid DNA. Nox1 protein expression showed similar elevation in all core-transfected samples with an average fold change in expression of 3.02±0.09 compared to control-transfected cells. Nox4 expression increased ~2.5-fold in transfectants with 1.0 and 2.0µg of core compared to control plasmid transfected cells (see **Figure 1a–d**). Both Nox1 and Nox4 mRNA expression was elevated with core, with Nox1 mRNA levels elevated by 45.7±7.25%, and 38.57±4.69% with 0.5µg and 1.0µg of core, respectively ($p<0.05$ vs. control). Nox1 mRNA with 2.0µg of core was also elevated, although slightly less than at lower doses, by 27.49±1.89% ($p<0.05$). Nox4 mRNA did not increase significantly (see **Figure 1e-f**).

Nox enzymes produce $O_2^{\cdot -}$ that can dismutate to H_2O_2 in a reaction catalyzed by SOD. H_2O_2 can further be detoxified by catalase or GSH-Px to produce water. Nox activity in the form of $O_2^{\cdot -}$ generation was quantified by cytochrome c reduction in Huh-7 cells transfected with HCV core or control vector (2µg/2.872cm^2) for 48 hours. Cytochrome c reduction measured after reaction for 30 minutes produced a 61.86±2.99% ($p<0.001$) increase in core-transfected cells compared to control cells not treated with DPI (see **Figure 2a**). Treatment with 10µM DPI significantly decreased cytochrome c reduction in both control and HCV core transfected cells, corresponding to decreases from 1.00±0.03 to 0.22±0.01 folds and 1.62±0.03 to 0.18±0.03 folds, respectively ($p<0.001$ for control and HCV core transfected cells, see **Figure 2b**). Upon extension of the reaction time from 30 minutes to 60 minutes, fold change in cytochrome c reduction increased to 4.63±0.05 in core transfected cells ($p<0.001$ vs. untreated control cells). Furthermore, treatment with 10µM DPI significantly decreased cytochrome c reduction in HCV core transfected cells ($p<0.001$). Measurement of H_2O_2 generation by fluorescent detection of HVA dimerization after 120 minutes yielded 56.32±10.19% more H_2O_2 with HCV core decreasing to near baseline at 0.97±0.17 –fold control with 10µM DPI (see **Figure 2c**).

3.2 Stable expression of HCV core upregulates Nox levels in hepatocytes

Huh-7 cells that were stably transfected with core plasmid, or empty vector, were selected for neomycin resistance with G418, and Nox levels were examined. Western blotting of whole cell lysates confirmed core protein expression, and Nox4 bands ranging

in size from 37kDa to above 115kDa were observed. The predicted size of the full length Nox4 protein, consisting of 578 amino acids, is 67kDa. Bands corresponding to 67kDa were only observed in stable core cells. A number of additional bands of both higher and lower molecular weight were also observed in hepatocytes expressing core, but not control cells. Nox protein levels in stable cells expressing core protein were overall significantly higher when compared to controls cells, corresponding to a 3.32±0.24 higher fold change in intensity (see **Figure 3a-b**). In addition, Nox1 and Nox4 mRNA levels were examined. Changes in Nox1 mRNA were not statistically significant in the core-expressing cells compared to controls. However, core cell clones 33.72±7.94% more Nox4 mRNA ($p<0.05$) compared to controls (see **Figure 3c-d**).

Nox enzyme activity, assessed by cytochrome c reduction, was 10-fold higher with core compared to controls (1.00±0.017 vs. 10.01±0.106, $p<0.001$). Furthermore, this elevation was reduced to undetectable levels by treatment with 10μM DPI during the 60 minute reaction time (see **Figure 3e**). Hydrogen peroxide production measured by HVA assay for 90 minutes showed an approximate 2-fold increase over controls. Furthermore, this increase was reduced to near baseline levels (1.09±0.17 vs. 1.00±0.008, $p<0.001$) upon treatment with 10μM DPI (see **Figure 3f**). In contrast, hydrogen peroxide production measured over 120 minutes, although also catalase-inhibitable, did not decrease with DPI treatment in controls or core-expressing cells (data not shown).

3.3 HCV core and Nox4 can localize to the nucleus and/or perinuclear space

To determine the localization of HCV core and Nox4 in stable core cells, immunofluorescence and subcellular fractionation were performed. As indicated by the replication cycle of HCV, core protein is readily detectible in the cytoplasm of hepatocytes by immunofluorescence (see **Figure 4a**). However, core protein exhibits a degree of overlap with the nuclear envelope protein, lamin A/C. Immunofluorescence detection of Nox4 protein showed a clear increase in the presence of core compared to control cells not expressing core, in addition to cytoplasmic staining in control and core-expressing cells. Furthermore, Nox4 showed staining in perinuclear and nuclear regions, a feature that was detected less frequently in the control cells (see **Figure 4b**). Western blotting analysis of subcellular fractions from core-expressing cells showed an elevation in Nox4 protein within the nuclear fraction and the corresponding whole cell lysate (WCL) (see **Figure 5a-b**). Furthermore, PCNA was elevated, between 45–50% higher than controls, in the cytoplasm and WCL. The nuclear fraction showed ~80% higher expression of PCNA with core versus the control fraction. In contrast, the post-nuclear fraction that contained fibrillarin (marker) showed ~80% less PCNA compared to the control cell post-nuclear fraction (see **Figure 5c**). Qualitatively, activated NF-κB heterodimer (~105kDa) was elevated in the cytoplasmic and nuclear fractions with constitutive expression of core protein compared to control. As was observed with PCNA, expression of activated NF-κB was primarily absent from the post-nuclear fraction in the presence of core. Collectively, these results show Nox4 can localizes to the nuclear region of core-expressing hepatocytes

that correlate with activation of cellular responses consistent with elevated ROS, such as NF-κB signaling and DNA synthesis and/or repair.

3.4 HCV core elevates DNA damage markers through Nox protein

The ratio of phosphorylated H2A.X (H2A.X-γ) versus non-phosphorylated H2A.X (H2A.X) was used as a primary indicator of DNA damage consistent with formation of double-stranded breaks in the DNA (see **Figure 6a-b**). Constitutive expression of core protein produced a 62% higher fold change in DNA damage compared to controls (1.62±0.05 versus 1.00±0.05, respectively, $p<0.001$). One hour of treatment with the flavoprotein inhibitor DPI at a final concentration of 10μM, or an equal volume of water solvent as a control, decreased DNA damage significantly (see **Figure 6c**). Hypoxia inducible factor 1α (HIF-1α) and H2AX-γ ratios were assessed by densitometry in the presence and absence of DPI. With respect to HIF-1α levels, treatment with solvent produced a small increase in protein expression, although not statistically significant. In contrast, treatment with DPI nearly diminished the HIF-1α signal, from 1.29±0.10 fold higher than control to 0.33±0.01-fold lower ($p=0.007$) than solvent-treated controls (see **Figure 6d**). Without DPI, H2A.X-γ levels of core-expressing cells treated with solvent exhibited a 2.09±0.18 –fold increase versus control cells (1.00±0.04, $p<0.001$). Treatment with DPI reduced H2A.X-γ levels from 2.08-fold higher than solvent-treated controls to 0.74±0.10-fold control ($p<0.001$), corresponding to a decrease below baseline levels (see **Figure 6e**).

To assess the ability of the novel Nox-specific inhibitor VAS-2870 (Enzo Life Sciences) to decrease Nox enzyme activity that causes DNA damage, SOD-inhibitable cytochrome c reduction was measured in lysed hepatocytes with and without core expression at three time points: 45 minutes, 60 minutes, and 75 minutes (see **Figure 7**). After 45 minutes, Nox activity was significantly higher in solvent treated core cells versus control, corresponding to an increase of 2.79±0.00 versus 1.00±0.07, respectively ($p<0.001$). DPI was capable of inhibiting Nox enzyme activity, however the percent inhibition in both control and core lysates was approximately 35% versus their respective solvent-treated samples (not statistically significant). In contrast, treatment with VAS-2870 at final concentrations between 5 and 20μM significantly reduced enzyme activity by approximately 1.3-fold ($p<0.001$). However, larger fluctuations in average fold change were observed with higher concentrations of VAS-2870; a final concentration of 5μM was sufficient to reduce enzyme activity (see **Figure 7a**). At 60 minutes, enzyme activity in solvent-treated core cells was 48.0±16.0% higher than controls, although this increase was not statistically significant. As was the case with the 45 minute reaction, treatment with 10μM DPI reduced control cell enzyme activity by ~40.00±14.42% ($p<0.05$). In contrast, DPI treatment of core cells did not decrease enzyme activity as efficiently nor as consistently as was observed at 45 minutes, corresponding to a 16.00±24.98% reduction. However, treatment with VAS-2870 at a final concentration of 5μM reduced Nox activity to levels 52% below solvent-treated control cell baseline ($p<0.05$). Higher concentrations

of VAS-2870 (10 and 20μM) also decreased Nox activity below solvent-treated baseline by 44.00±4.00% and 60.00±4.00%, respectively ($p<0.05$). With respect to control cells treated with VAS-2870, enzyme activity was 90% abolished by treatment with 20μM VAS-2870 (see **Figure 7b**). Lastly, after a 75 minute reaction, cytochrome c reduction remained elevated in solvent-treated core cells versus controls, corresponding to a 1.87±0.03–fold increase ($p<0.001$). As described above, treatment with DPI reduced enzyme activity between 35–45% in control and core-expressing cells, versus corresponding solvent-treated cells (significant in core cells, $p<0.05$). Similar to observations in the 60 minute reaction, treatment of HCV core cells with VAS-2870, particularly at a concentration of 5μM, decreased Nox activity 20% below solvent-treated control cells at 75 minutes ($p<0.001$). VAS-2870 treatment of control cells also significantly reduced Nox activity, although only between 45 and 55% below solvent-treated controls (see **Figure 7c**). In summary, core-expressing cells exhibited markers of oxidative stress consistent with lesions in the DNA and hypoxic signaling frequently observed in cancer. Furthermore, inhibition of flavoproteins with DPI decreased DNA damage markers, and observed elevation in oxidative stress was reducible by the novel Nox-inhibitor, VAS-2870.

Chapter 4 - Discussion and conclusion

A causal link between CHC and progression of severe liver diseases such as cirrhosis and HCC has been widely recognized since the identification of HCV in the late 1980's. Many studies have aimed to elucidate the pathogenic mechanisms of individual viral proteins, as well as by infectious virus production using cell culture systems and animal models. However, as is the case in many viral pathogenesis studies, the availability of sufficiently susceptible animal models and virus-producing cell culture systems present significant limitations in the field. Such limitations are not nonexistent in the field of HCV research. In particular, variations in disease progression and response to treatment are believed to be, at least in part, dependent on viral genotype. Currently, the most widely used models to study the pathogenic mechanisms of HCV utilize the JFH-1 strain of genotype 2a. However, a recent epidemiological study revealed that genotype 1 accounts for 46% of global HCV infections.[139] Furthermore, studies show that genotype prevalence varies with geographic distribution. For example, although genotype 1 is the most prevalent globally, Gower, *et al.* reported that genotype 4 is responsible for 93.1% of cases in Egypt and between 60.0 – 96.8% of cases in central sub-Saharan Africa, northern Africa, and the Middle East. With respect to genotype 1a, the highest prevalence occurs in Andean South America, North America, and various countries such as the Philippines, the Dominican Republic, Peru, and Puerto Rico.[139]

The role of genotype in predicting progression to HCC is widely debated, in part due to the lack of studies with sufficient sample size that account for confounding variables such as alcohol consumption and other comorbidities including metabolic conditions, all of which may impact the overall results. However, a hallmark pathogenic feature of chronic HCV infection, identified as early as 1996, is increased oxidative stress.[102] Several sources of elevated oxidative stress induced by CHC have been identified, including Nox proteins. This study establishes a framework for the elucidation of the role that genotype 1a core protein plays in carcinogenesis through upregulation of Nox enzyme expression and generation of ROS. The greater implication is to investigate the therapeutic benefit of targeting the decrease of specific Nox proteins to mitigate disease progression.

Upregulation of Nox4 and 1 was observed after 48 hours of transient transfection of human hepatocytes with plasmid containing genotype 1a (H77 strain) core protein coding sequence or control plasmid. Upon transfection of varying dose combinations of core-containing and control plasmid DNA, each totaling 4µg, revealed elevations in Nox1 and 4 protein expression and Nox1 mRNA levels. Overall, among the concentrations tested (0–2µg), optimal expression of Nox4 and 1 was achieved with 2µg of core-containing plasmid, corresponding to a 2.5-fold increase in Nox4 protein and a 3.0-fold increase in Nox1 protein levels versus control, whereas 0.5µg was sufficient to achieve maximal Nox1 protein increase (see **Figure 1**). Although the data in Figure 1 represents one assessment of Nox protein expression with core, two additional experiments (data not shown) confirm

elevation in Nox4 expression ranging from 2.0–3.0-fold higher with HCV core. Corresponding elevations in Nox1 expression were also confirmed with transfection of 2µg of core plasmid, although the fold elevations in Nox1 tended to vary from one experiment to another (e.g., 1.5–2.0-fold higher than controls versus the data shown in **Figure 1**). Interestingly, Nox4 mRNA levels did not increase significantly, suggesting potential translational or post-translational regulation of Nox4 protein level. Additional experiments revealed elevation of Nox4 mRNA 48 hours after transient transfection with core plasmid DNA, confirming elevation by approximately 50% over control. Despite this intriguing elevation in Nox4 mRNA, further experiments are required to determine the significance of Nox4 mRNA alterations or lack of significant alterations by HCV core in these cells. In contrast, Nox1 mRNA levels presented in **Figure 1** showed statistically significant elevation with 2µg of core, in addition to lower plasmid levels. Two additional experiments also confirmed Nox1 elevation (approximately 50%) with transient transfection of HCV core construct for 48 hours.

To determine Nox enzyme activity, superoxide production was assayed by cytochrome c reduction in permeabilized cells after transient transfection with genotype 1a core for 48 hours. In this study, Nox activity measurements lasting 30 and 60 minutes produced a 1.6 and 4.6-fold increase with core that was statistically significant, respectively (see **Figure 2**). Furthermore, treatment with DPI significantly reduced Nox activity in hepatocytes transfected with core. However, the reduction of ferricytochrome c (Fe^{3+}) to ferrocytochrome c (Fe^{2+}) by superoxide is inherently susceptible to a wide variety of electron carriers that can also reduce cytochrome c and DPI is not a specific inhibitor of Nox1 or Nox4. To partly address this, we demonstrated that the cytochrome c assay is sensitive to SOD with the addition of DPI that inhibits flavoproteins and is commonly used to inhibit Nox enzymes. However, additional flavoproteins are capable of producing superoxide, such as complex I of the ETC in the mitochondria, and thus the assay must be complemented with other techniques to conclusively prove that elevated superoxide with HCV core is the result of Nox proteins. Additional methods to detect superoxide production resulting from elevated Nox proteins would be beneficial in future studies, such as non-chemiluminescent methods like HPLC detection of dihydroethidium (DHE) fluorescence, or electron spin resonance using various probes.[140]

Another method to monitor elevations in oxidative stress is production of H_2O_2.[141] It is speculated that Nox4 can produce H_2O_2 in addition to superoxide, and as superoxide would dismutate to H_2O_2 inside the cell and diffuse across the plasma membrane, H_2O_2 production that is catalase-inhibitable can be measured extracellularly and used as an indicator of intracellular ROS production.[142] Indeed, 48 hours after transient transfection with core, 120 minutes of HVA reaction monitoring dimerization into a fluorogenic compound in the presence of HRP demonstrated elevated fluorescence by genotype 1a HCV core. A 56% elevation in catalase-inhibitable H_2O_2 production was observed and its

reduction by 60% with DPI treatment suggested elevated H_2O_2 resulting from a DPI-sensitive factor upon expression of the core protein (see **Figure 2**).

Taken together, these results suggest that genotype 1a core protein is sufficient to elevate both Nox4 and Nox1 protein levels, in addition to increasing production of ROS 48 hours post-transfection. However, investigation of Nox expression assessed in two separate experiments at additional time points, including 24, 72, and 96 hours after transfection (data not shown), revealed variable alterations in Nox protein levels, and thus require additional studies to clarify the time course of changes in Nox gene expression. One factor that may be attributable to differences in protein expression is the assessment of transfection efficiency. Assessment of transfection efficiency via co-transfection with a β-galactosidase plasmid, driven by an SV40 promoter with subsequent collection for β-galactosidase activity, revealed 2–3-fold elevations in enzyme activity with core protein, compared to empty vector control transfections. One study suggested that HCV core protein exhibits a trans-activating effect on the SV40 promoter, thus enhancing β-galactosidase expression, measured at levels up to 5-fold higher than control plasmid.[143] An additional factor that can impact consistent delivery of plasmid DNA to cells is the transfection method. In this study, co-precipitation of plasmid DNA with calcium phosphate was used. Indeed, this method has been reported to produce variations in transfection efficiency and cell survival that are affected by slight changes in the concentration of plasmid DNA and the duration of exposure to the co-precipitate.[144] To further confirm time-dependent expression of Nox proteins and mRNA, further studies need to be conducted using additional transfection techniques (liposome or electroporation) and other reporter systems to assess transfection efficiency. For example, transfection of Huh-7 cells with HCV-ribozyme construct of genotype 1b (CG1b) containing the secreted alkaline phosphatase (SEAP) reporter gene has been used to measure transfection efficiency by SEAP enzyme activity in cell culture media.[145]

To address any variations in the transfection efficiencies between experiments, stable cell clones that constitutively express core were used for the remainder of experiments. One potential benefit of constitutive expression of core protein, is that it could mirror the chronic HCV core expression in hepatitis C patients who experience severe disease progression in the liver after infection. Indeed, constitutive expression of core produced significant elevations in Nox4 protein expression (see **Figure 3a-b**). Of note is that additional high and low molecular weight bands, not seen upon transient transfection, were observed above 115kDa and below 49kDa (see **Figure 3a**). Based on the complete sequence of Nox4, 9 possible isoforms can be produced by alternative splicing with corresponding molecular weights ranging from 6 to 64kDa.[146] However, the tissue-specific expression profiles for each of the 9 possible isoforms has not been fully elucidated, nor have their individual relevance in oxidative stress and the development of HCC been completely determined, particularly in hepatocytes. The appearance of bands above and

below ~67kDa, the predicted molecular weight of full-length Nox4, may represent isoforms corresponding to Nox4D or Nox4E, whose predicted molecular weights are 32 and 28kDa, respectively. Upon recent evidence suggesting that Nox4D, corresponding to isoform 4, localizes to the nucleus of vascular smooth muscle cells (VSMCs) when Nox4 is over-expressed, it is reasonable that overexpression of Nox4 by core may result in alternative splicing of full-length Nox4 mRNA to produce additional isoforms with differing properties. In fact, Nox4D and E isoforms lack all but one hydrophobic transmembrane domain in the N-terminus, and are thus considered "soluble" Nox4 enzymes. However, Nox4D exhibited comparable enzyme activity to full-length Nox4, whereas Nox4E did not produce elevated ROS.[92] Although this result is intriguing, further studies would be required to characterize the array of bands observed in this experiment to validate such a conclusion.

Constitutive expression of core protein corresponded with a significant elevation in Nox4 mRNA levels ($p<0.05$). Similar findings have been described by our lab with genomic JFH1 RNA, but these results were not observed with subgenomic RNA.[93] However, in this study, Nox1 mRNA elevation was not significant. Furthermore, de Mochel *et al.* described elevated superoxide activity and hydrogen peroxide production with genotype 2a virus-producing Huh-7 cells. In this study, constitutive expression of 1a core produced 10-fold higher Nox activity that decreased upon treatment with DPI. Similar to observations with transient expression of core, H_2O_2 showed a 2-fold increase with core. This elevation in ROS production was reduced to near or below baseline levels with DPI treatment, suggesting that core expression is sufficient to increase ROS generation as previously described.[71,96,147]

The ability of ROS to induce oxidative damage is dependent on the subcellular location as well as context in which it is generated. For example, ROS production in contained phagocytic vesicles provides valuable antimicrobial functions. However, the biological functions of ROS, as the name implies, are not limited to the destruction of microbes. In addition, ROS contribute to various widespread physiological functions, including alteration of intracellular signaling that are capable of dictating progression through the cell cycle as well as induction of adaptations to cellular metabolism. Given this potential, ROS production is tightly regulated, and it may be hypothesized that ROS produced in excess may be harmful, particularly in close proximity to sensitive DNA-containing organelles, such as the nucleus. Therefore, since this study has thus far shown that expression of core protein is sufficient to elevate oxidative stress, the subcellular localization of both core protein, and Nox4 were investigated.

Some authors report that core protein is observable in the nucleus of hepatocytes, despite the cytoplasmic life cycle of HCV.[148–150] It was shown that trafficking of core protein to the nucleus likely occurs under the direction of a nuclear localization signal (NLS) in the form of three polypeptide stretches rich in hydrophobic arginine and lysine

sequences.[151] This observation of nuclear localization is confirmed by our study (see **Figure 4a**). Although not solely localized in the nucleus, core protein was largely observed throughout the cytoplasm, and in the perinuclear space by immunofluorescence. As Nox4 expression is increased with core, the sub-cellular localization of Nox4 with constitutive expression of core may constitute, at least in part, the basis for oxidative damage to key molecules like DNA in hepatocytes that would contribute to tumor formation. Consistent with our Western Blotting results, Nox4 fluorescence was elevated with constitutive expression of core protein. In addition, punctate nuclear staining of Nox4 was visible with continuous expression of core protein (see **Figure 4b**). Subcellular location, however, was not confirmed by immunofluorescence after transient transfection with core protein. These results are intriguing as they align with the hypothesis that expression of core protein induces Nox4 upregulation, as well as localization to the nucleus.

To confirm our IF results, subcellular fractionation was performed on stable core-expressing cells (see **Figure 5**). Interestingly, core protein was observed in the nuclear and post-nuclear fractions, consistent with our IF results in Figure 4. Additionally, elevation of Nox4 (approximately 20%) in the nucleus was observed with the predicted molecular weight of ~67kDa representing full length Nox4. Interestingly, lower molecular weight isoforms were also observed in nuclear and post-nuclear fractions as well as the WCL. Previous descriptions of Nox4 isoforms indicate that N-glycosylation of isoforms D and E can produce bands between 28 and 39kDa.[92] Goyal *et al.* report that isoforms D and E of Nox4 are 17% more likely to be found in the nucleus compared to Nox1. Furthermore, ROS generation was significantly higher in Nox4D transfected human pulmonary epithelial (A549) cells, and inhibition of glycosylation by administration of tunicamycin reduced ROS generation. Although these results are intriguing, several weaknesses exist in the sub-cellular fractionation results presented in this study. Most importantly, the fractionation results are representative of one experiment, and thus would need to be repeated several more times to conclusively confirm the IF results. Also, challenges were faced in selecting fractionation markers suitable for this application, as the core protein has been reported to alter the expression of a wide array of cellular proteins.[133]

Additional proteins for which expression was assessed in the presence of core after fractionation include PCNA and NF-κB. Interestingly, expression of PCNA was elevated in cytoplasmic and nuclear fractions, as well as in WCLs. As PCNA is a cell cycle regulator essential for DNA synthesis and repair, elevated expression in the nucleus is suggestive of increased proliferation and/or genotoxicity. Indeed, PCNA was increased by approximately 80% in the core expressing nuclear fraction compared to the nuclear control fraction (see **Figure 5c**). Interestingly, one study found that transgenic core mice homozygous dominant for peroxisome proliferator-activated receptor alpha (PPARα), a transcription factor and major regulator of lipid metabolism, developed severe hepatic steatosis and HCC. Furthermore, examination of the livers of these mice showed significant

elevation of PCNA in the nuclei by immunohistochemistry and in whole liver lysates analyzed by Western Blotting.[152] Another transcription factor that core protein interacts with is NF-κB, for which its activation by core is associated with hepatocyte proliferation through induction of TGF-α signaling.[153] However, activation of NF-κB is one of several proliferative mechanisms through which core protein may contribute to the generation of HCC. In the cytoplasm, the NF-κB heterodimer consisting of subunits RelA (p65) and p50 remain bound to its regulatory subunit IκBα. Upon activation, IκB kinase (IKK) phosphorylates the regulatory subunit causing its release, which then allows migration of the 105kDa heterodimer to the nucleus were it acts as a transcription factor for a number of target genes.[154] In this study, constitutive expression of core protein did not produce elevations of NF-κB at the predicted molecular weight, 65kDa (see **Figure 5a**). Although, higher molecular weight bands, ~100kDa, were observed despite protein denaturation and separation by SDS-PAGE prior to Western Blotting. The assessment of NF-κB activation by Western Blotting has been regarded as cautionary, and indeed these results are evidence of this.[155] Although the apparent elevation in intensity of bands migrating near 100kDa are an intriguing finding, they require repetition to validate the results. Furthermore, use of additional techniques such as electrophoretic mobility shift assay (EMSA) to show NF-κB-DNA interactions in nuclear fractions, or ELISA reporter assay, chromatin immunoprecipitation (ChIP) assay, or IKB degradation are required to show activation.

The connection between HCV and the development of HCC has been widely demonstrated. The pathogenic mechanisms by which HCC develops upon infection with HCV, however, is still not fully understood. Specifically, many studies indicate conflicting effects resulting from expression of HCV proteins, specifically non-structural proteins 3 and 5a, and structural core protein. For example, authors report differential effects of core on the tumor suppressor protein p53, each suggesting either enhanced activation or suppression of p53.[124,125,156,157] Additional studies add controversy to the subject of core protein and apoptosis, with some indicating an inhibitory effect of core on TNF-α induced apoptosis, and others more recently suggesting that core interacts with TNF receptor 1 (TNFR1) promoting apoptosis.[158,159]

Nonetheless, the correlation between enhanced DNA damage and oxidative stress with HCV has been widely observed *in vitro* and *in vivo*.[104,106,147] Therefore, to elucidate the role of upregulated Nox proteins by core on DNA damage, lesions in the DNA were investigated. One of the most severe types of damage in DNA is strand breakage, and in particular DSBs. Phosphorylation of H2A.X serves as an important indicator of DSBs, and its presence is necessary for damage recognition by repair proteins. In this study, DNA damage was measured by the ratio of phosphorylated-to-non-phosphorylated H2AX (H2AX-γ/H2AX) protein in the presence of core. We showed that stable expression of core protein was sufficient to increase H2AX-γ/H2AX by 1.6–2.0-fold when compared to stable cells transfected with empty vector (see **Figure 6**). This finding is consistent with the

observation of enhanced H2AX-γ in pre-neoplastic lesions within the livers of HCC patients, the majority of which were infected with CHC.[160] Furthermore, a study published this year showed similar elevation in H2AX-γ with infectious genotype 1a HCV in post-attachment primary hepatocytes (PPHs).[161] Interestingly, the observed elevation in H2AX-γ was shown to be mediated by loss of nuclear phosphatase and tensin homologue (PTEN), an important tumor suppressor protein that exhibits an array of downstream effects, such as mediating genome stability and centromere stabilization. Ultimately, PTEN protein serves as an important regulator of cell cycle control, and its loss in the nucleus is associated with more aggressive cancers.[162–164]

To demonstrate the role of Nox proteins in DNA damage, we showed that administration of DPI yielded a significant reduction in H2AX-γ/H2AX protein levels. One question raised by these findings, evident in **Figure 6c**, is the increase in baseline H2AX expression of control cells after treatment with DPI. Although this elevation does not alter the overall trend as quantified in **Figure 6e**, further analysis is required to explain the effect of DPI on H2AX levels in stable control-transfected cells. Another interesting finding that occurred with constitutive expression of core, was the apparent decrease in core protein expression after DPI treatment. However, further studies are required to identify and characterize interactions between DPI and translation of core protein.

The additive effects of DNA damage over time are certainly capable of altering cell cycle regulation, promoting cell transformation. In addition, disruption of cellular metabolism and angiogenesis are also frequently observed hallmarks of cancer.[165] One such alteration in cellular metabolism is the tendency of cancer cells to shift from aerobic to anaerobic glycolysis, termed the "Warburg Effect".[166] This shift in glycolytic metabolism has been attributed to mitochondrial dysfunction, an effect observed in cancers.[167] Furthermore, tumor development requires a constant supply of oxygen from blood vessels to support continuous growth and proliferation, typically followed by invasion and metastasis. Increased proliferation is not only energetically consuming, but can promote hypoxic signaling, a common feature in cancer cells. Hypoxia-inducible factor 1 (HIF-1) is a heterodimeric protein that is essential in the maintenance of cellular oxygen metabolism. Both subunits of HIF-1, termed α and β, are expressed under conditions of normal oxygen, but the HIF-1α subunit is readily degraded when oxygen is available, preventing nuclear translocation. Under hypoxic conditions HIF-1α is stabilized, allowing subsequent translocation to the nucleus where the HIF-1 heterodimer can act as a transcription factor. It has been reported that infection with HCV is capable of stabilizing the HIF-1α subunit by activation of transcription factors, including NF-κB, that promote angiogenesis and the development of HCC.[168]

In our study, HIF-1α protein expression was not significantly elevated with core expression. However, upon treatment with DPI for 60 minutes, HIF-1α levels decreased significantly in core cell clones (see **Figure 6d**). These results suggest that inhibition of

flavoproteins, such as Nox proteins, may decrease excessive hypoxic signaling that contributes to angiogenesis and initiation of metastatic events in the presence of genotype 1a HCV core. Although these results are encouraging, further studies are required to investigate the effect of Nox inhibition on other signaling molecules involved in the hypoxic response pathway.

Recent development of the novel Nox-specific inhibitor VAS-2870 has significantly advanced the study of Nox proteins, as it may serve as a potential therapeutic agent to reduce oxidative stress derived from Nox protein overexpression. The current standard for specific inhibition of Nox proteins is through gene knockdown experiments that involve using small interfering RNAs (siRNAs). However, proper validation of their effectiveness at silencing Nox expression at the RNA and protein level could be challenging.[169] Therefore, we investigated the ability of VAS-2870 to inhibit Nox activity via the cytochrome c reduction assay. Interestingly, we found that administration of VAS-2870 at final concentrations of 5, 10, and 20µm produced significant decreases in cytochrome c reduction measured at three different time points in hepatocyte lysates prepared from Huh-7 cells constitutively expressing core (see **Figure 7**). The inhibition of cytochrome c reduction in core-expressing cells by VAS-2870 was significantly better than inhibition with DPI, which supports the hypothesis that the source of oxidative stress measured by the Nox activity assay are Nox proteins, rather than other flavoproteins such as xanthine oxidase. In fact, ROS generation in vascular smooth muscle cells after treatment with 10µM VAS-2870 was significantly inhibited without disruption of xanthine oxidase activity, further indicating that VAS-2870 is Nox-specific.[170] Even more encouraging is that lower concentrations of VAS-2870 (down to 5µM final) could reduce Nox activity, in addition to the sustained reduction over time, a desirable quality in validating the use of chemical inhibitors for therapeutic purposes. These results are extremely encouraging and offer additive validation of the role Nox-derived ROS generation serves in HCV-associated oxidative stress. The commercial availability of VAS-2870 makes it an exciting compound to employ in the study of Nox proteins, which most certainly warrants further consideration.

Altogether, the findings of this study provide supporting evidence that genotype 1a HCV core protein is, on its own, sufficient to elevate Nox1 and 4 at multiple levels, including mRNA, protein, and enzyme activity. Furthermore, results suggest that core protein is also capable of inducing DSBs in DNA, possibly promoting oncogenic changes which would contribute to the development of HCC. Although many of the findings in this study require further validation and development, they may serve as a step toward increasing our understanding of how a single virus can be responsible for such global health concern. In contrast to chronic hepatitis B, for which there is now a vaccine, no vaccine against HCV has been developed. Recently developed antiviral drug treatments have shown promise with respect to increasing rates of sustained virological response, but

evidence also suggests that HCC can develop in individuals with pre-treatment liver disease who clear the virus after treatment.[171,172] Therefore, the development of anti-oxidative stress therapies may present a viable option in cancer prevention, specifically for those with chronic hepatitis C infection, whose primary metabolic detoxifying organ, the liver, could act as a ticking time bomb.

Chapter 5 - References

1 Szabó E, Lotz G, Páska C, Kiss A, Schaff Z. Viral hepatitis: new data on hepatitis C infection. *Pathol Oncol Res POR* 2003; **9**: 215–221.

2 Armstrong GL, Wasley A, Simard EP, McQuillan GM, Kuhnert WL, Alter MJ. The prevalence of hepatitis C virus infection in the United States, 1999 through 2002. *Ann Intern Med* 2006; **144**: 705–714.

3 Tong MJ, el-Farra NS, Reikes AR, Co RL. Clinical outcomes after transfusion-associated hepatitis C. *N Engl J Med* 1995; **332**: 1463–1466.

4 Wasley A, Kruszon-Moran D, Kuhnert W, Simard EP, Finelli L, McQuillan G *et al.* The prevalence of hepatitis B virus infection in the United States in the era of vaccination. *J Infect Dis* 2010; **202**: 192–201.

5 Mohd Hanafiah K, Groeger J, Flaxman AD, Wiersma ST. Global epidemiology of hepatitis C virus infection: New estimates of age-specific antibody to HCV seroprevalence. *Hepatology* 2013; **57**: 1333–1342.

6 Brown RS, Gaglio PJ. Scope of worldwide hepatitis C problem. *Liver Transpl* 2003; **9**: S10–S13.

7 Averhoff FM, Glass N, Holtzman D. Global Burden of Hepatitis C: Considerations for Healthcare Providers in the United States. *Clin Infect Dis* 2012; **55**: S10–S15.

8 El-Serag HB. Epidemiology of viral hepatitis and hepatocellular carcinoma. *Gastroenterology* 2012; **142**: 1264–1273.e1.

9 Kim DY, Ahn SH, Han K-H. Emerging Therapies for Hepatitis C. *Gut Liver* 2014; **8**: 471–479.

10 Cunningham M, Foster GR. Efficacy and safety of telaprevir in patients with genotype 1 hepatitis C infection. *Ther Adv Gastroenterol* 2012; **5**: 139–151.

11 Marino Z, van Bommel F, Forns X, Berg T. New concepts of sofosbuvir-based treatment regimens in patients with hepatitis C. *Gut* 2013. doi:10.1136/gutjnl-2013-305771.

12 Lawitz E, Mangia A, Wyles D, Rodriguez-Torres M, Hassanein T, Gordon SC *et al.* Sofosbuvir for previously untreated chronic hepatitis C infection. *N Engl J Med* 2013; **368**: 1878–1887.

13 Feld JJ, Hoofnagle JH. Mechanism of action of interferon and ribavirin in treatment of hepatitis C. *Nature* 2005; **436**: 967–972.

14 Jemal A, Siegel R, Ward E, Hao Y, Xu J, Thun MJ. Cancer statistics, 2009. *CA Cancer J Clin* 2009; **59**: 225–249.

15 Altekruse SF, McGlynn KA, Reichman ME. Hepatocellular Carcinoma Incidence, Mortality, and Survival Trends in the United States From 1975 to 2005. *J Clin Oncol* 2009; **27**: 1485–1491.

16 McMahon BJ. The natural history of chronic hepatitis B virus infection. *Hepatol Baltim Md* 2009; **49**: S45–55.

17 Choo QL, Kuo G, Weiner AJ, Overby LR, Bradley DW, Houghton M. Isolation of a cDNA clone derived from a blood-borne non-A, non-B viral hepatitis genome. *Science* 1989; **244**: 359–362.

18 Tobler LH, Busch MP. History of posttransfusion hepatitis. *Clin Chem* 1997; **43**: 1487–1493.

19 Griffin SDC. A conserved basic loop in hepatitis C virus p7 protein is required for amantadine-sensitive ion channel activity in mammalian cells but is dispensable for localization to mitochondria. *J Gen Virol* 2004; **85**: 451–461.

20 Griffin SDC, Beales LP, Clarke DS, Worsfold O, Evans SD, Jaeger J *et al.* The p7 protein of hepatitis C virus forms an ion channel that is blocked by the antiviral drug, Amantadine. *FEBS Lett* 2003; **535**: 34–38.

21 Sakai A, Claire MS, Faulk K, Govindarajan S, Emerson SU, Purcell RH *et al.* The p7 polypeptide of hepatitis C virus is critical for infectivity and contains functionally important genotype-specific sequences. *Proc Natl Acad Sci* 2003; **100**: 11646–11651.

22 Santolini E, Pacini L, Fipaldini C, Migliaccio G, Monica N. The NS2 protein of hepatitis C virus is a transmembrane polypeptide. *J Virol* 1995; **69**: 7461–7471.

23 Yamaga AK. Membrane Topology of the Hepatitis C Virus NS2 Protein. *J Biol Chem* 2002; **277**: 33228–33234.

24 Pieroni L, Santolini E, Fipaldini C, Pacini L, Migliaccio G, La Monica N. In vitro study of the NS2-3 protease of hepatitis C virus. *J Virol* 1997; **71**: 6373–6380.

25 Lindenbach BD, Rice CM. Unravelling hepatitis C virus replication from genome to function. *Nature* 2005; **436**: 933–938.

26 Foy E, Li K, Wang C, Sumpter R, Ikeda M, Lemon SM *et al.* Regulation of interferon regulatory factor-3 by the hepatitis C virus serine protease. *Science* 2003; **300**: 1145–1148.

27 Elazar M, Liu P, Rice CM, Glenn JS. An N-terminal amphipathic helix in hepatitis C virus (HCV) NS4B mediates membrane association, correct localization of replication complex proteins, and HCV RNA replication. *J Virol* 2004; **78**: 11393–11400.

28 Egger D, Wölk B, Gosert R, Bianchi L, Blum HE, Moradpour D *et al.* Expression of hepatitis C virus proteins induces distinct membrane alterations including a candidate viral replication complex. *J Virol* 2002; **76**: 5974–5984.

29 Lundin M, Monné M, Widell A, Von Heijne G, Persson MAA. Topology of the membrane-associated hepatitis C virus protein NS4B. *J Virol* 2003; **77**: 5428–5438.

30 Tanji Y, Kaneko T, Satoh S, Shimotohno K. Phosphorylation of hepatitis C virus-encoded nonstructural protein NS5A. *J Virol* 1995; **69**: 3980–3986.

31 Brass V, Bieck E, Montserret R, Wölk B, Hellings JA, Blum HE *et al.* An amino-terminal amphipathic alpha-helix mediates membrane association of the hepatitis C virus nonstructural protein 5A. *J Biol Chem* 2002; **277**: 8130–8139.

32 Tellinghuisen TL, Marcotrigiano J, Gorbalenya AE, Rice CM. The NS5A protein of hepatitis C virus is a zinc metalloprotein. *J Biol Chem* 2004; **279**: 48576–48587.

33 Tellinghuisen TL, Marcotrigiano J, Rice CM. Structure of the zinc-binding domain of an essential component of the hepatitis C virus replicase. *Nature* 2005; **435**: 374–379.

34 Schmidt-Mende J, Bieck E, Hugle T, Penin F, Rice CM, Blum HE *et al.* Determinants for Membrane Association of the Hepatitis C Virus RNA-dependent RNA Polymerase. *J Biol Chem* 2001; **276**: 44052–44063.

35 Lohmann V, Körner F, Koch J, Herian U, Theilmann L, Bartenschlager R. Replication of subgenomic hepatitis C virus RNAs in a hepatoma cell line. *Science* 1999; **285**: 110–113.

36 Bartenschlager R, Lohmann V, Penin F. The molecular and structural basis of advanced antiviral therapy for hepatitis C virus infection. *Nat Rev Microbiol* 2013; **11**: 482–496.

37 Chatel-Chaix L, Bartenschlager R. Dengue Virus- and Hepatitis C Virus-Induced Replication and Assembly Compartments: the Enemy Inside--Caught in the Web. *J Virol* 2014; **88**: 5907–5911.

38 Hundt J. Post-translational modifications of hepatitis C viral proteins and their biological significance. *World J Gastroenterol* 2013; **19**: 8929.

39 Scheel TKH, Rice CM. Understanding the hepatitis C virus life cycle paves the way for highly effective therapies. *Nat Med* 2013; **19**: 837–849.

40 Zeisel MB, Fofana I, Fafi-Kremer S, Baumert TF. Hepatitis C virus entry into hepatocytes: molecular mechanisms and targets for antiviral therapies. *J Hepatol* 2011; **54**: 566–576.

41 Romero-Brey I, Merz A, Chiramel A, Lee J-Y, Chlanda P, Haselman U *et al.* Three-dimensional architecture and biogenesis of membrane structures associated with hepatitis C virus replication. *PLoS Pathog* 2012; **8**: e1003056.

42 Lukavsky PJ. Structure and function of HCV IRES domains. *Virus Res* 2009; **139**: 166–171.

43 Pestova TV, Shatsky IN, Fletcher SP, Jackson RJ, Hellen CU. A prokaryotic-like mode of cytoplasmic eukaryotic ribosome binding to the initiation codon during internal translation initiation of hepatitis C and classical swine fever virus RNAs. *Genes Dev* 1998; **12**: 67–83.

44 Lindenbach BD, Meuleman P, Ploss A, Vanwolleghem T, Syder AJ, McKeating JA *et al.* Cell culture-grown hepatitis C virus is infectious in vivo and can be recultured in vitro. *Proc Natl Acad Sci U S A* 2006; **103**: 3805–3809.

45 Atkins E, Tatineni R, Li H, Gretch D, Harris M, Griffin S. The stability of secreted, acid-labile H77/JFH-1 hepatitis C virus (HCV) particles is altered by patient isolate genotype 1a p7 sequences. *Virology* 2014; **448**: 117–124.

46 Whitfield T, Miles AJ, Scheinost JC, Offer J, Wentworth Jr P, Dwek RA *et al.* The influence of different lipid environments on the structure and function of the hepatitis C virus p7 ion channel protein. *Mol Membr Biol* 2011; **28**: 254–264.

47 Chew CF, Vijayan R, Chang J, Zitzmann N, Biggin PC. Determination of Pore-Lining Residues in the Hepatitis C Virus p7 Protein. *Biophys J* 2009; **96**: L10–L12.

48 Hurtado-Nedelec M, Makni-Maalej K, Gougerot-Pocidalo M-A, Dang PM-C, El-Benna J. Assessment of priming of the human neutrophil respiratory burst. *Methods Mol Biol Clifton NJ* 2014; **1124**: 405–412.

49 Overstreet JM, Samarakoon R, Meldrum KK, Higgins PJ. Redox control of p53 in the transcriptional regulation of TGF-β1 target genes through SMAD cooperativity. *Cell Signal* 2014. doi:10.1016/j.cellsig.2014.02.017.

50 Brandes RP, Weissmann N, Schröder K. Redox-mediated signal transduction by cardiovascular Nox. *J Mol Cell Cardiol* 2014. doi:10.1016/j.yjmcc.2014.02.006.

51 Masella R, Di Benedetto R, Varì R, Filesi C, Giovannini C. Novel mechanisms of natural antioxidant compounds in biological systems: involvement of glutathione and glutathione-related enzymes. *J Nutr Biochem* 2005; **16**: 577–586.

52 Yamamoto Y, Yamashita S, Fujisawa A, Kokura S, Yoshikawa T. Oxidative Stress in Patients with Hepatitis, Cirrhosis, and Hepatoma Evaluated by Plasma Antioxidants. *Biochem Biophys Res Commun* 1998; **247**: 166–170.

53 Scholz RW, Graham KS, Gumpricht E, Reddy CC. Mechanism of Interaction of Vitamin E and Glutathione in the Protection against Membrane Lipid Peroxidation. *Ann N Y Acad Sci* 1989; **570**: 514–517.

54 Meister A. Mitochondrial changes associated with glutathione deficiency. *Biochim Biophys Acta* 1995; **1271**: 35–42.

55 Lenton KJ, Sané AT, Therriault H, Cantin AM, Payette H, Wagner JR. Vitamin C augments lymphocyte glutathione in subjects with ascorbate deficiency. *Am J Clin Nutr* 2003; **77**: 189–195.

56 Farias MS, Budni P, Ribeiro CM, Parisotto EB, Santos CEI, Dias JF *et al.* Antioxidant supplementation attenuates oxidative stress in chronic hepatitis C patients. *Gastroenterol Hepatol* 2012; **35**: 386–394.

57 Abdalla MY, Ahmad IM, Spitz DR, Schmidt WN, Britigan BE. Hepatitis C virus-core and non structural proteins lead to different effects on cellular antioxidant defenses. *J Med Virol* 2005; **76**: 489–497.

58 Levent G, Ali A, Ahmet A, Polat EC, Aytaç C, Ayşe E *et al.* Oxidative stress and antioxidant defense in patients with chronic hepatitis C patients before and after pegylated interferon alfa-2b plus ribavirin therapy. *J Transl Med* 2006; **4**: 25.

59 Tandara L, Salamunic I. Iron metabolism: current facts and future directions. *Biochem Medica* 2012; **22**: 311–328.

60 Shan Y, Lambrecht RW, Bonkovsky HL. Association of hepatitis C virus infection with serum iron status: analysis of data from the third National Health and Nutrition Examination Survey. *Clin Infect Dis Off Publ Infect Dis Soc Am* 2005; **40**: 834–841.

61 Nishina S, Hino K, Korenaga M, Vecchi C, Pietrangelo A, Mizukami Y *et al.* Hepatitis C virus-induced reactive oxygen species raise hepatic iron level in mice by reducing hepcidin transcription. *Gastroenterology* 2008; **134**: 226–238.

62 Miura K, Taura K, Kodama Y, Schnabl B, Brenner DA. Hepatitis C virus-induced oxidative stress suppresses hepcidin expression through increased histone deacetylase activity. *Hepatol Baltim Md* 2008; **48**: 1420–1429.

63 Fierbinţeanu-Braticevici C, Mohora M, Creţoiu D, Creţoiu S, Petrişor A, Usvat R *et al.* Role of oxidative stress in the pathogenesis of chronic hepatitis C (CHC). *Romanian J Morphol Embryol Rev Roum Morphol Embryol* 2009; **50**: 407–412.

64 Madill J, Arendt BM, Aghdassi E, Therapondos G, Lilly L, Chow C-W *et al.* Hepatic Lipid Peroxidation and Antioxidant Micronutrients in Hepatitis Virus C Liver Recipients With and Without Disease Recurrence. *Transplant Proc* 2009; **41**: 3800–3805.

65 Korenaga M, Wang T, Li Y, Showalter LA, Chan T, Sun J *et al.* Hepatitis C virus core protein inhibits mitochondrial electron transport and increases reactive oxygen species (ROS) production. *J Biol Chem* 2005; **280**: 37481–37488.

66 Ivanov A, Bartosch B, Smirnova O, Isaguliants M, Kochetkov S. HCV and Oxidative Stress in the Liver. *Viruses* 2013; **5**: 439–469.

67 Okuda M, Li K, Beard M, Showalter L, Scholle F, Lemon S *et al.* Mitochondrial injury, oxidative stress, and antioxidant gene expression are induced by hepatitis C virus core protein. *Gastroenterology* 2002; **122**: 366–375.

68 Piccoli C, Scrima R, Quarato G, D'Aprile A, Ripoli M, Lecce L *et al.* Hepatitis C virus protein expression causes calcium-mediated mitochondrial bioenergetic dysfunction and nitro-oxidative stress. *Hepatology* 2007; **46**: 58–65.

69 Ando M, Korenaga M, Hino K, Ikeda M, Kato N, Nishina S *et al.* Mitochondrial electron transport inhibition in full genomic hepatitis C virus replicon cells is restored by reducing viral replication: HCV and mitochondrial electron transport. *Liver Int* 2008; **28**: 1158–1166.

70 Wang T, Campbell RV, Yi MK, Lemon SM, Weinman SA. Role of Hepatitis C virus core protein in viral-induced mitochondrial dysfunction. *J Viral Hepat* 2010; **17**: 784–793.

71 Li Y, Boehning DF, Qian T, Popov VL, Weinman SA. Hepatitis C virus core protein increases mitochondrial ROS production by stimulation of Ca2+ uniporter activity. *FASEB J* 2007; **21**: 2474–2485.

72 Choi J, Forman HJ, Ou J, Lai MMC, Seronello S, Nandipati A. Redox modulation of the hepatitis C virus replication complex is calcium dependent. *Free Radic Biol Med* 2006; **41**: 1488–1498.

73 Schwer B, Ren S, Pietschmann T, Kartenbeck J, Kaehlcke K, Bartenschlager R *et al.* Targeting of hepatitis C virus core protein to mitochondria through a novel C-terminal localization motif. *J Virol* 2004; **78**: 7958–7968.

74 Lu Y, Cederbaum AI. CYP2E1 and oxidative liver injury by alcohol. *Free Radic Biol Med* 2008; **44**: 723–738.

75 Rigamonti C, Mottaran E, Reale E, Rolla R, Cipriani V, Capelli F *et al.* Moderate alcohol consumption increases oxidative stress in patients with chronic hepatitis C. *Hepatol Baltim Md* 2003; **38**: 42–49.

76 Nakai K, Tanaka H, Hanada K, Ogata H, Suzuki F, Kumada H *et al.* Decreased Expression of Cytochromes P450 1A2, 2E1, and 3A4 and Drug Transporters Na+-Taurocholate-Cotransporting Polypeptide, Organic Cation Transporter 1, and Organic Anion-Transporting Peptide-C Correlates with the Progression of Liver Fibrosis in Chronic Hepatitis C Patients. *Drug Metab Dispos* 2008; **36**: 1786–1793.

77 Wen F, Abdalla MY, Aloman C, Xiang J, Ahmad IM, Walewski J *et al.* Increased prooxidant production and enhanced susceptibility to glutathione depletion in HepG2 cells co-expressing HCV core protein and CYP2E1. *J Med Virol* 2004; **72**: 230–240.

78 Otani K, Korenaga M, Beard MR, Li K, Qian T, Showalter LA *et al.* Hepatitis C virus core protein, cytochrome P450 2E1, and alcohol produce combined mitochondrial injury and cytotoxicity in hepatoma cells. *Gastroenterology* 2005; **128**: 96–107.

79 Geller DA, Lowenstein CJ, Shapiro RA, Nussler AK, Di Silvio M, Wang SC *et al.* Molecular cloning and expression of inducible nitric oxide synthase from human hepatocytes. *Proc Natl Acad Sci U S A* 1993; **90**: 3491–3495.

80 Machida K, Cheng KT-H, Sung VM-H, Lee KJ, Levine AM, Lai MMC. Hepatitis C virus infection activates the immunologic (type II) isoform of nitric oxide synthase and thereby enhances DNA damage and mutations of cellular genes. *J Virol* 2004; **78**: 8835–8843.

81 Majano PL, García-Monzón C, López-Cabrera M, Lara-Pezzi E, Fernández-Ruiz E, García-Iglesias C *et al.* Inducible nitric oxide synthase expression in chronic viral hepatitis. Evidence for a virus-induced gene upregulation. *J Clin Invest* 1998; **101**: 1343–1352.

82 Kane JM 3rd, Shears LL 2nd, Hierholzer C, Ambs S, Billiar TR, Posner MC. Chronic hepatitis C virus infection in humans: induction of hepatic nitric oxide synthase and proposed mechanisms for carcinogenesis. *J Surg Res* 1997; **69**: 321–324.

83 Vodovotz Y, Kim PKM, Bagci EZ, Ermentrout GB, Chow CC, Bahar I *et al.* Inflammatory modulation of hepatocyte apoptosis by nitric oxide: in vivo, in vitro, and in silico studies. *Curr Mol Med* 2004; **4**: 753–762.

84 Lambeth JD. NOX enzymes and the biology of reactive oxygen. *Nat Rev Immunol* 2004; **4**: 181–189.

85 Pollock JD, Williams DA, Gifford MA, Li LL, Du X, Fisherman J *et al.* Mouse model of X-linked chronic granulomatous disease, an inherited defect in phagocyte superoxide production. *Nat Genet* 1995; **9**: 202–209.

86 Bureau C. Nonstructural 3 Protein of Hepatitis C Virus Triggers an Oxidative Burst in Human Monocytes via Activation of NADPH Oxidase. *J Biol Chem* 2001; **276**: 23077–23083.

87 Thoren F, Romero A, Lindh M, Dahlgren C, Hellstrand K. A hepatitis C virus-encoded, nonstructural protein (NS3) triggers dysfunction and apoptosis in lymphocytes: role of NADPH oxidase-derived oxygen radicals. *J Leukoc Biol* 2004; **76**: 1180–1186.

88 Tacke RS, Tosello-Trampont A, Nguyen V, Mullins DW, Hahn YS. Extracellular hepatitis C virus core protein activates STAT3 in human monocytes/macrophages/dendritic cells via an IL-6 autocrine pathway. *J Biol Chem* 2011; **286**: 10847–10855.

89 Corzo CA, Cotter MJ, Cheng P, Cheng F, Kusmartsev S, Sotomayor E *et al.* Mechanism regulating reactive oxygen species in tumor-induced myeloid-derived suppressor cells. *J Immunol Baltim Md 1950* 2009; **182**: 5693–5701.

90 Von Lohneysen K, Noack D, Wood MR, Friedman JS, Knaus UG. Structural Insights into Nox4 and Nox2: Motifs Involved in Function and Cellular Localization. *Mol Cell Biol* 2009; **30**: 961–975.

91 Von Lohneysen K, Noack D, Hayes P, Friedman JS, Knaus UG. Constitutive NADPH Oxidase 4 Activity Resides in the Composition of the B-loop and the Penultimate C Terminus. *J Biol Chem* 2012; **287**: 8737–8745.

92 Goyal P, Weissmann N, Rose F, Grimminger F, Schäfers HJ, Seeger W *et al.* Identification of novel Nox4 splice variants with impact on ROS levels in A549 cells. *Biochem Biophys Res Commun* 2005; **329**: 32–39.

93 De Mochel NSR, Seronello S, Wang SH, Ito C, Zheng JX, Liang TJ *et al.* Hepatocyte NAD(P)H oxidases as an endogenous source of reactive oxygen species during hepatitis C virus infection. *Hepatology* 2010; **52**: 47–59.

94 Spencer NY, Yan Z, Boudreau RL, Zhang Y, Luo M, Li Q *et al.* Control of Hepatic Nuclear Superoxide Production by Glucose 6-Phosphate Dehydrogenase and NADPH Oxidase-4. *J Biol Chem* 2011; **286**: 8977–8987.

95 Anilkumar N, Jose GS, Sawyer I, Santos CXC, Sand C, Brewer AC *et al.* A 28-kDa Splice Variant of NADPH Oxidase-4 Is Nuclear-Localized and Involved in Redox Signaling in Vascular Cells. *Arterioscler Thromb Vasc Biol* 2013; **33**: e104–e112.

96 Boudreau HE, Emerson SU, Korzeniowska A, Jendrysik MA, Leto TL. Hepatitis C Virus (HCV) Proteins Induce NADPH Oxidase 4 Expression in a Transforming Growth Factor - Dependent Manner: a New Contributor to HCV-Induced Oxidative Stress. *J Virol* 2009; **83**: 12934–12946.

97 Fisher AB. Redox Signaling Across Cell Membranes. *Antioxid Redox Signal* 2009; **11**: 1349–1356.

98 Neuman MG, Schmilovitz-Weiss H, Hilzenrat N, Bourliere M, Marcellin P, Trepo C *et al.* Markers of Inflammation and Fibrosis in Alcoholic Hepatitis and Viral Hepatitis C. *Int J Hepatol* 2012; **2012**: 1–10.

99 Taniguchi H, Kato N, Otsuka M, Goto T, Yoshida H, Shiratori Y *et al.* Hepatitis C virus core protein upregulates transforming growth factor-beta 1 transcription. *J Med Virol* 2004; **72**: 52–59.

100 Burdette D, Haskett A, Presser L, McRae S, Iqbal J, Waris G. Hepatitis C virus activates interleukin-1 via caspase-1-inflammasome complex. *J Gen Virol* 2012; **93**: 235–246.

101 Negash AA, Ramos HJ, Crochet N, Lau DTY, Doehle B, Papic N *et al.* IL-1β Production through the NLRP3 Inflammasome by Hepatic Macrophages Links Hepatitis C Virus Infection with Liver Inflammation and Disease. *PLoS Pathog* 2013; **9**: e1003330.

102 De Maria N, Colantoni A, Fagiuoli S, Liu GJ, Rogers BK, Farinati F *et al.* Association between reactive oxygen species and disease activity in chronic hepatitis C. *Free Radic Biol Med* 1996; **21**: 291–295.

103 Machida K, Cheng KT-N, Sung VM-H, Shimodaira S, Lindsay KL, Levine AM *et al.* Hepatitis C virus induces a mutator phenotype: Enhanced mutations of immunoglobulin and protooncogenes. *Proc Natl Acad Sci* 2004; **101**: 4262–4267.

104 Shimoda R, Nagashima M, Sakamoto M, Yamaguchi N, Hirohashi S, Yokota J *et al.* Increased formation of oxidative DNA damage, 8-hydroxydeoxyguanosine, in human livers with chronic hepatitis. *Cancer Res* 1994; **54**: 3171–3172.

105 Schwarz KB, Kew M, Klein A, Abrams RA, Sitzmann J, Jones L *et al.* Increased hepatic oxidative DNA damage in patients with hepatocellular carcinoma. *Dig Dis Sci* 2001; **46**: 2173–2178.

106 Farinati F, Cardin R, Degan P, De Maria N, Floyd RA, Van Thiel DH *et al.* Oxidative DNA damage in circulating leukocytes occurs as an early event in chronic HCV infection. *Free Radic Biol Med* 1999; **27**: 1284–1291.

107 Kitada T, Seki S, Iwai S, Yamada T, Sakaguchi H, Wakasa K. In situ detection of oxidative DNA damage, 8-hydroxydeoxyguanosine, in chronic human liver disease. *J Hepatol* 2001; **35**: 613–618.

108 Ichiba M, Maeta Y, Mukoyama T, Saeki T, Yasui S, Kanbe T *et al.* Expression of 8-hydroxy-2'-deoxyguanosine in chronic liver disease and hepatocellular carcinoma. *Liver Int Off J Int Assoc Study Liver* 2003; **23**: 338–345.

109 Lloyd DR, Carmichael PL, Phillips DH. Comparison of the Formation of 8-Hydroxy-2‘-deoxyguanosine and Single- and Double-Strand Breaks in DNA Mediated by Fenton Reactions. *Chem Res Toxicol* 1998; **11**: 420–427.

110 Niles JC, Wishnok JS, Tannenbaum SR. Peroxynitrite-induced oxidation and nitration products of guanine and 8-oxoguanine: Structures and mechanisms of product formation. *Nitric Oxide* 2006; **14**: 109–121.

111 Valavanidis A, Vlachogianni T, Fiotakis C. 8-hydroxy-2’ -deoxyguanosine (8-OHdG): A critical biomarker of oxidative stress and carcinogenesis. *J Environ Sci Health Part C Environ Carcinog Ecotoxicol Rev* 2009; **27**: 120–139.

112 Ramana CV, Boldogh I, Izumi T, Mitra S. Activation of apurinic/apyrimidinic endonuclease in human cells by reactive oxygen species and its correlation with their adaptive response to genotoxicity of free radicals. *Proc Natl Acad Sci U S A* 1998; **95**: 5061–5066.

113 Higgs MR, Chouteau P, Lerat H. ‘Liver let die’: oxidative DNA damage and hepatotropic viruses. *J Gen Virol* 2014; **95**: 991–1004.

114 Menoni H, Hoeijmakers JHJ, Vermeulen W. Nucleotide excision repair-initiating proteins bind to oxidative DNA lesions in vivo. *J Cell Biol* 2012; **199**: 1037–1046.

115 Costa R. The eukaryotic nucleotide excision repair pathway. *Biochimie* 2003; **85**: 1083–1099.

116 Chapman JR, Taylor MRG, Boulton SJ. Playing the End Game: DNA Double-Strand Break Repair Pathway Choice. *Mol Cell* 2012; **47**: 497–510.

117 San Filippo J, Sung P, Klein H. Mechanism of eukaryotic homologous recombination. *Annu Rev Biochem* 2008; **77**: 229–257.

118 Mao Z, Bozzella M, Seluanov A, Gorbunova V. Comparison of nonhomologous end joining and homologous recombination in human cells. *DNA Repair* 2008; **7**: 1765–1771.

119 Mao Z, Bozzella M, Seluanov A, Gorbunova V. DNA repair by nonhomologous end joining and homologous recombination during cell cycle in human cells. *Cell Cycle Georget Tex* 2008; **7**: 2902–2906.

120 Machida K, McNamara G, Cheng KT-H, Huang J, Wang C-H, Comai L *et al.* Hepatitis C virus inhibits DNA damage repair through reactive oxygen and nitrogen species and by interfering with the ATM-NBS1/Mre11/Rad50 DNA repair pathway in monocytes and hepatocytes. *J Immunol Baltim Md 1950* 2010; **185**: 6985–6998.

121 Bae I. BRCA1 Induces Antioxidant Gene Expression and Resistance to Oxidative Stress. *Cancer Res* 2004; **64**: 7893–7909.

122 Le Page F, Randrianarison V, Marot D, Cabannes J, Perricaudet M, Feunteun J *et al.* BRCA1 and BRCA2 are necessary for the transcription-coupled repair of the oxidative 8-oxoguanine lesion in human cells. *Cancer Res* 2000; **60**: 5548–5552.

123 Lai C-K, Jeng K-S, Machida K, Cheng Y-S, Lai MMC. Hepatitis C virus NS3/4A protein interacts with ATM, impairs DNA repair and enhances sensitivity to ionizing radiation. *Virology* 2008; **370**: 295–309.

124 Lu W, Lo SY, Chen M, Wu K j, Fung YK, Ou JH. Activation of p53 tumor suppressor by hepatitis C virus core protein. *Virology* 1999; **264**: 134–141.

125 Otsuka M, Kato N, Lan K, Yoshida H, Kato J, Goto T *et al*. Hepatitis C virus core protein enhances p53 function through augmentation of DNA binding affinity and transcriptional ability. *J Biol Chem* 2000; **275**: 34122–34130.

126 Siavoshian S, Abraham JD, Kieny MP, Schuster C. HCV core, NS3, NS5A and NS5B proteins modulate cell proliferation independently from p53 expression in hepatocarcinoma cell lines. *Arch Virol* 2004; **149**: 323–336.

127 Yamanaka T, Kodama T, Doi T. Subcellular localization of HCV core protein regulates its ability for p53 activation and p21 suppression. *Biochem Biophys Res Commun* 2002; **294**: 528–534.

128 Kao C-F, Chen S-Y, Chen J-Y, Wu Lee Y-H. Modulation of p53 transcription regulatory activity and post-translational modification by hepatitis C virus core protein. *Oncogene* 2004; **23**: 2472–2483.

129 Dubourdeau M, Miyamura T, Matsuura Y, Alric L, Pipy B, Rousseau D. Infection of HepG2 cells with recombinant adenovirus encoding the HCV core protein induces p21(WAF1) down-regulation -- effect of transforming growth factor beta. *J Hepatol* 2002; **37**: 486–492.

130 Jung EY, Lee MN, Yang HY, Yu D, Jang KL. The repressive activity of hepatitis C virus core protein on the transcription of p21(waf1) is regulated by protein kinase A-mediated phosphorylation. *Virus Res* 2001; **79**: 109–115.

131 Honda M, Kaneko S, Shimazaki T, Matsushita E, Kobayashi K, Ping L *et al*. Hepatitis C virus core protein induces apoptosis and impairs cell-cycle regulation in stably transformed chinese hamster ovary cells. *Hepatology* 2000; **31**: 1351–1359.

132 Park KJ, Choi SH, Koh MS, Kim DJ, Yie SW, Lee SY *et al*. Hepatitis C virus core protein potentiates c-Jun N-terminal kinase activation through a signaling complex involving TRADD and TRAF2. *Virus Res* 2001; **74**: 89–98.

133 Kasprzak A, Adamek A. Role of hepatitis C virus proteins (C, NS3, NS5A) in hepatic oncogenesis. *Hepatol Res* 2008; **38**: 1–26.

134 Lo SY, Selby M, Tong M, Ou JH. Comparative studies of the core gene products of two different hepatitis C virus isolates: two alternative forms determined by a single amino acid substitution. *Virology* 1994; **199**: 124–131.

135 Suzuki T, Aizaki H, Murakami K, Shoji I, Wakita T. Molecular biology of hepatitis C virus. *J Gastroenterol* 2007; **42**: 411–423.

136 Seres T, Knickelbein RG, Warshaw JB, Johnston RB. The Phagocytosis-Associated Respiratory Burst in Human Monocytes Is Associated with Increased Uptake of Glutathione. *J Immunol* 2000; **165**: 3333–3340.

137 Chen K, Kirber MT, Xiao H, Yang Y, Keaney JF. Regulation of ROS signal transduction by NADPH oxidase 4 localization. *J Cell Biol* 2008; **181**: 1129–1139.

138 Zhang L, Nguyen MVC, Lardy B, Jesaitis AJ, Grichine A, Rousset F *et al*. New insight into the Nox4 subcellular localization in HEK293 cells: First monoclonal antibodies against Nox4. *Biochimie* 2011; **93**: 457–468.

139 Gower E, Estes C, Blach S, Razavi-Shearer K, Razavi H. Global epidemiology and genotype distribution of the hepatitis C virus infection. *J Hepatol* 2014; **61**: S45–S57.

140 Dikalov S, Griendling KK, Harrison DG. Measurement of Reactive Oxygen Species in Cardiovascular Studies. *Hypertension* 2007; **49**: 717–727.

141 Ruch W, Cooper PH, Baggiolini M. Assay of H_2O_2 production by macrophages and neutrophils with homovanillic acid and horse-radish peroxidase. *J Immunol Methods* 1983; **63**: 347–357.

142 Nisimoto Y, Diebold BA, Cosentino-Gomes D, Lambeth JD. Nox4: A Hydrogen Peroxide-Generating Oxygen Sensor. *Biochemistry (Mosc)* 2014; **53**: 5111–5120.

143 Liu M, Liu Y, Cheng J, Zhang S-L, Wang L, Shao Q *et al*. Transactivating effect of hepatitis C virus core protein: a suppression subtractive hybridization study. *World J Gastroenterol WJG* 2004; **10**: 1746–1749.

144 Kingston RE, Chen CA, Rose JK. Calcium Phosphate Transfection. In: Ausubel FM, Brent R, Kingston RE, Moore DD, Seidman JG, Smith JA *et al.* (eds). *Current Protocols in Molecular Biology*. John Wiley & Sons, Inc.: Hoboken, NJ, USA, 2003http://doi.wiley.com/10.1002/0471142727.mb0901s63 (accessed 7 Nov2014).

145 Kato T, Date T, Murayama A, Morikawa K, Akazawa D, Wakita T. Cell culture and infection system for hepatitis C virus. *Nat Protoc* 2006; **1**: 2334–2339.

146 Q9NPH5 - NOX4_HUMAN. Univers. Protein Resour. UniProt. http://www.uniprot.org/uniprot/Q9NPH5 (accessed 19 Nov2014).

147 Machida K, Cheng KT-H, Lai C-K, Jeng K-S, Sung VM-H, Lai MMC. Hepatitis C virus triggers mitochondrial permeability transition with production of reactive oxygen species, leading to DNA damage and STAT3 activation. *J Virol* 2006; **80**: 7199–7207.

148 Liu Q, Tackney C, Bhat RA, Prince AM, Zhang P. Regulated processing of hepatitis C virus core protein is linked to subcellular localization. *J Virol* 1997; **71**: 657–662.

149 Suzuki R, Matsuura Y, Suzuki T, Ando A, Chiba J, Harada S *et al*. Nuclear localization of the truncated hepatitis C virus core protein with its hydrophobic C terminus deleted. *J Gen Virol* 1995; **76 (Pt 1)**: 53–61.

150 Yasui K, Wakita T, Tsukiyama-Kohara K, Funahashi SI, Ichikawa M, Kajita T *et al.* The native form and maturation process of hepatitis C virus core protein. *J Virol* 1998; **72**: 6048–6055.

151 Chang SC, Yen JH, Kang HY, Jang MH, Chang MF. Nuclear localization signals in the core protein of hepatitis C virus. *Biochem Biophys Res Commun* 1994; **205**: 1284–1290.

152 Tanaka N, Moriya K, Kiyosawa K, Koike K, Gonzalez FJ, Aoyama T. PPARα activation is essential for HCV core protein–induced hepatic steatosis and hepatocellular carcinoma in mice. *J Clin Invest* 2008. doi:10.1172/JCI33594.

153 Sato Y, Kato J, Takimoto R, Takada K, Kawano Y, Miyanishi K *et al.* Hepatitis C virus core protein promotes proliferation of human hepatoma cells through enhancement of transforming growth factor alpha expression via activation of nuclear factor-kappaB. *Gut* 2006; **55**: 1801–1808.

154 McDonald PP, Bald A, Cassatella MA. Activation of the NF-kappaB pathway by inflammatory stimuli in human neutrophils. *Blood* 1997; **89**: 3421–3433.

155 Herkenham M, Rathore P, Brown P, Listwak SJ. Cautionary notes on the use of NF-κB p65 and p50 antibodies for CNS studies. *J Neuroinflammation* 2011; **8**: 141.

156 Hassan M, Ghozlan H, Abdel-Kader O. Activation of RB/E2F signaling pathway is required for the modulation of hepatitis C virus core protein-induced cell growth in liver and non-liver cells. *Cell Signal* 2004; **16**: 1375–1385.

157 Lee MN, Jung EY, Kwun HJ, Jun HK, Yu D-Y, Choi YH *et al.* Hepatitis C virus core protein represses the p21 promoter through inhibition of a TGF-beta pathway. *J Gen Virol* 2002; **83**: 2145–2151.

158 Zhu N, Khoshnan A, Schneider R, Matsumoto M, Dennert G, Ware C *et al.* Hepatitis C virus core protein binds to the cytoplasmic domain of tumor necrosis factor (TNF) receptor 1 and enhances TNF-induced apoptosis. *J Virol* 1998; **72**: 3691–3697.

159 Saito K, Meyer K, Warner R, Basu A, Ray RB, Ray R. Hepatitis C virus core protein inhibits tumor necrosis factor alpha-mediated apoptosis by a protective effect involving cellular FLICE inhibitory protein. *J Virol* 2006; **80**: 4372–4379.

160 Matsuda Y, Wakai T, Kubota M, Osawa M, Takamura M, Yamagiwa S *et al.* DNA damage sensor γ -H2AX is increased in preneoplastic lesions of hepatocellular carcinoma. *ScientificWorldJournal* 2013; **2013**: 597095.

161 Bao W, Florea L, Wu N, Wang Z, Banaudha K, Qian J *et al.* Loss of nuclear PTEN in HCV-infected human hepatocytes. *Infect Agent Cancer* 2014; **9**: 23.

162 Tachibana M, Shibakita M, Ohno S, Kinugasa S, Yoshimura H, Ueda S *et al.* Expression and prognostic significance of PTEN product protein in patients with esophageal squamous cell carcinoma. *Cancer* 2002; **94**: 1955–1960.

163 Zhou XP, Gimm O, Hampel H, Niemann T, Walker MJ, Eng C. Epigenetic PTEN silencing in malignant melanomas without PTEN mutation. *Am J Pathol* 2000; **157**: 1123–1128.

164 Zhou X-P, Loukola A, Salovaara R, Nystrom-Lahti M, Peltomäki P, de la Chapelle A *et al.* PTEN mutational spectra, expression levels, and subcellular localization in microsatellite stable and unstable colorectal cancers. *Am J Pathol* 2002; **161**: 439–447.

165 Hanahan D, Weinberg RA. Hallmarks of Cancer: The Next Generation. *Cell* 2011; **144**: 646–674.

166 Pavlides S, Vera I, Gandara R, Sneddon S, Pestell RG, Mercier I *et al.* Warburg Meets Autophagy: Cancer-Associated Fibroblasts Accelerate Tumor Growth and Metastasis *via* Oxidative Stress, Mitophagy, and Aerobic Glycolysis. *Antioxid Redox Signal* 2012; **16**: 1264–1284.

167 Simonnet H, Alazard N, Pfeiffer K, Gallou C, Béroud C, Demont J *et al.* Low mitochondrial respiratory chain content correlates with tumor aggressiveness in renal cell carcinoma. *Carcinogenesis* 2002; **23**: 759–768.

168 Nasimuzzaman M, Waris G, Mikolon D, Stupack DG, Siddiqui A. Hepatitis C virus stabilizes hypoxia-inducible factor 1alpha and stimulates the synthesis of vascular endothelial growth factor. *J Virol* 2007; **81**: 10249–10257.

169 Altenhöfer S, Kleikers PWM, Radermacher KA, Scheurer P, Rob Hermans JJ, Schiffers P *et al.* The NOX toolbox: validating the role of NADPH oxidases in physiology and disease. *Cell Mol Life Sci CMLS* 2012; **69**: 2327–2343.

170 Tenfreyhaus H, Huntgeburth M, Wingler K, Schnitker J, Baumer A, Vantler M *et al.* Novel Nox inhibitor VAS2870 attenuates PDGF-dependent smooth muscle cell chemotaxis, but not proliferation☆. *Cardiovasc Res* 2006; **71**: 331–341.

171 Chang K-C, Wu Y-Y, Hung C-H, Lu S-N, Lee C-M, Chiu K-W *et al.* Clinical-guide risk prediction of hepatocellular carcinoma development in chronic hepatitis C patients after interferon-based therapy. *Br J Cancer* 2013; **109**: 2481–2488.

172 Kobayashi S, Takeda T, Enomoto M, Tamori A, Kawada N, Habu D *et al.* Development of hepatocellular carcinoma in patients with chronic hepatitis C who had a sustained virological response to interferon therapy: a multicenter, retrospective cohort study of 1124 patients. *Liver Int Off J Int Assoc Study Liver* 2007; **27**: 186–191.

Chapter 6 - Figures

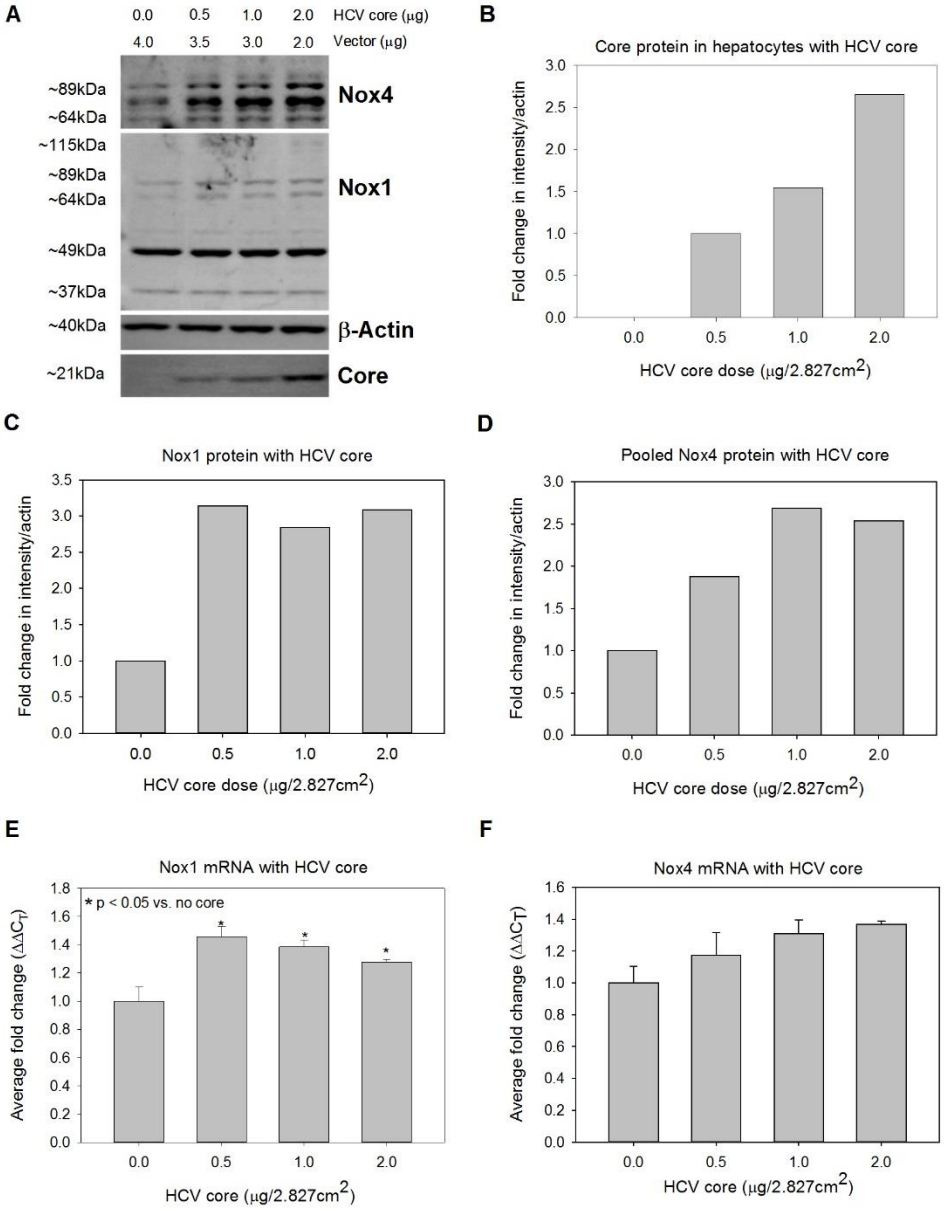

Figure 1. Nox expression with transient transfection of HCV core. (A) Western blotting on 10μL of whole cell lysate solubilized in 2x Laemmli buffer. Samples were run in duplicates on the same gel and incubated with antibodies for Nox proteins separately to avoid signal overlap due to insufficient reblot and/or antibody host similarity. Relative intensities were normalized with respect to β-Actin and fold change was calculated relative to the control transfected sample. (B) Core protein expression was assessed by normalization to samples transfected with 0.5μg of HCV core protein. (C) Nox1 expression as measured by the intensity of the bands between 64 and 89kDa relative to control. (D) Nox4 expression as determined by the additive intensity of the bands between 64 and 89kDa with appropriate normalization. Data in B, C, and D were normalized by β-actin bands and expressed as average fold change from respective controls, performed twice (E and F) Relative amounts of Nox1 and Nox4 mRNA levels were assessed by quantitative RT-PCR using GAPDH mRNA as a control (n=3).

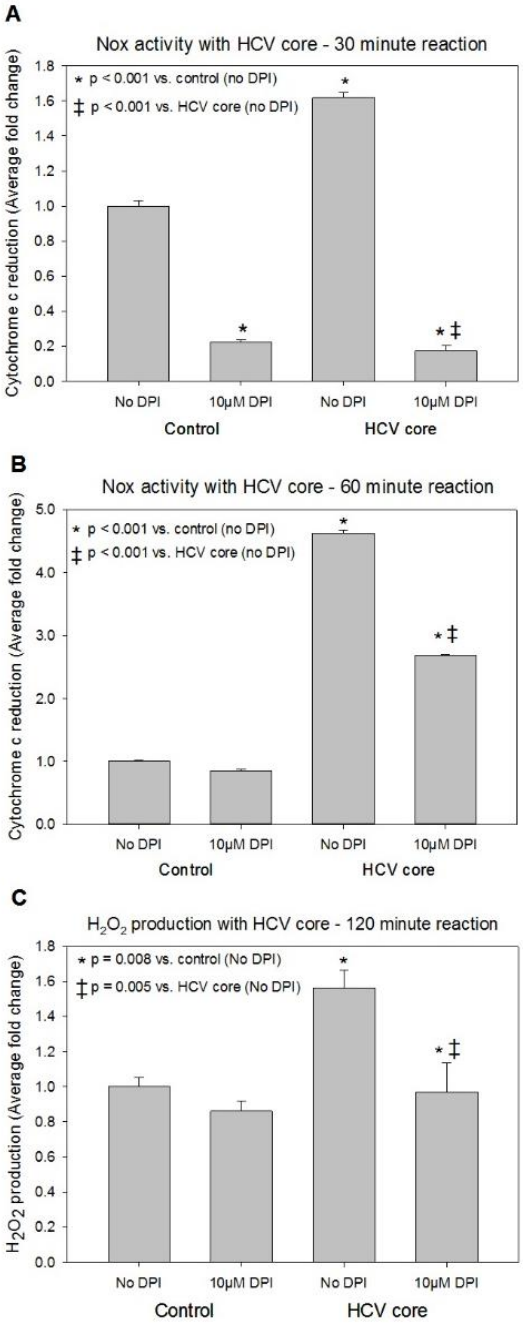

Figure 2. Nox activity and hydrogen peroxide levels in hepatocytes transiently expressing HCV core. Reduction of SOD-inhibitable cytochrome c was calculated by the change in absorbance at 550nm with reference at 540nm (n=3). Treatment with 10μM DPI, an inhibitor of flavoproteins including Nox enzymes, was used to test the source of elevations in Nox activity and hydrogen peroxide. (A) Nox activity, measured by absorbance after 30 minutes of SOD-inhibitable cytochrome c reduction in the presence of 10μM DPI or water solvent control. (B) Nox activity after 60 minutes of SOD-inhibitable cytochrome c reduction. (C) Hydrogen peroxide level measured by catalase-inhibitable HVA dimerization in the presence of HRP, measured at an excitation wavelength of 321nm and emission at 420nm.

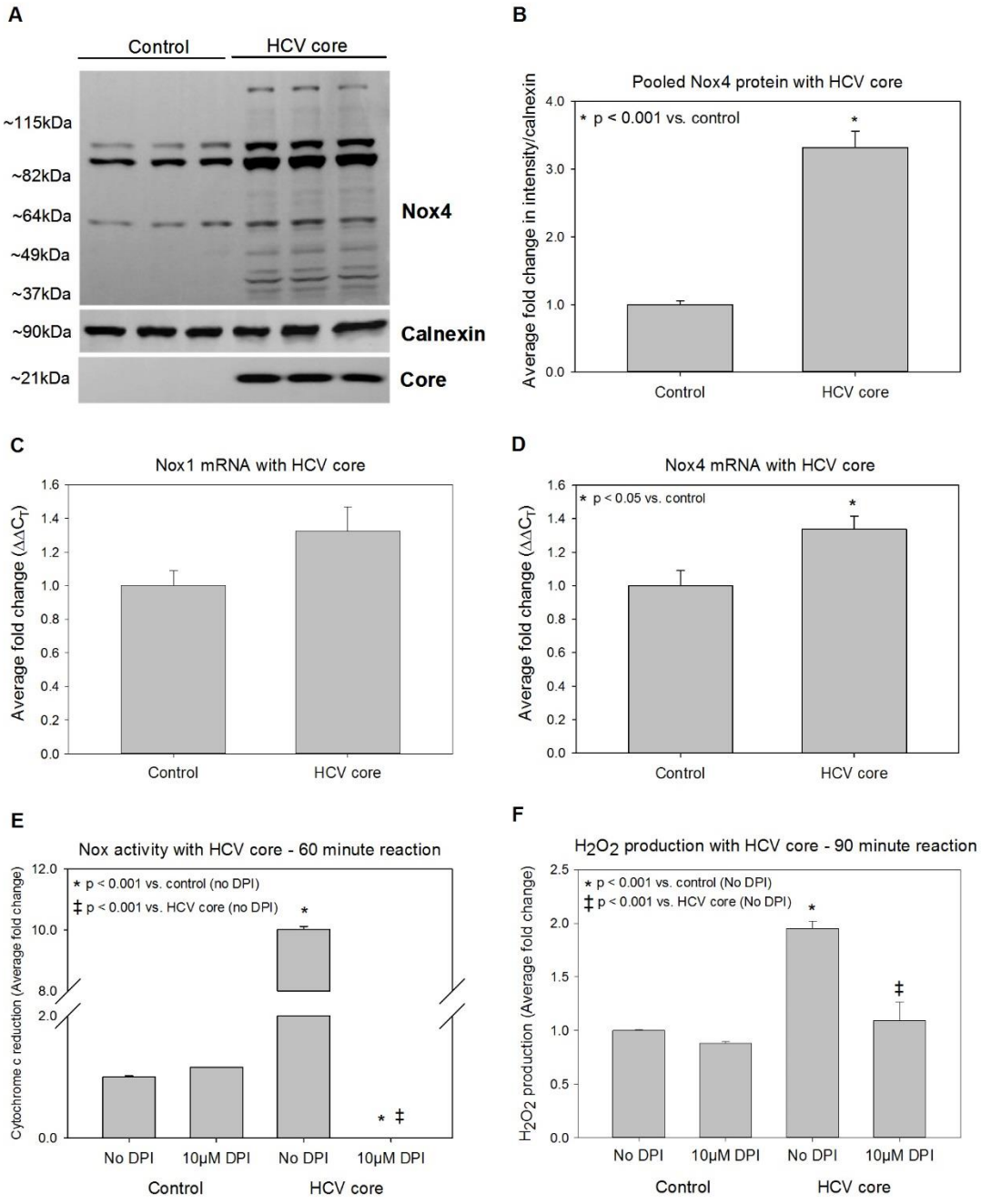

Figure 3. Nox protein, mRNA, and enzyme activity, and H_2O_2 levels in hepatocytes stably expressing HCV core. All experiments were conducted in triplicates. (A) Western blotting on 10μL of whole cell lysate solubilized in 2x Laemmli buffer and run in triplicates. Intensities were normalized by calnexin bands and expressed as average fold change from respective controls (B) Nox4 expression was calculated for each lane by densitometry analysis of all bands above 37kDa for control and HCV core expressing cells. (C and D) Relative amounts of Nox1 and Nox4 mRNA were assessed by quantitative RT-PCR using GAPDH mRNA as a control. (E) Nox activity was measured by SOD-inhibitable cytochrome c reduction after a 60 minute reaction. (F) Hydrogen peroxide was measured by catalase-inhibitable HVA dimerization in the presence of HRP, after a 90 minutes reaction measured at an excitation wavelength of 321nm and excitation at 420nm.

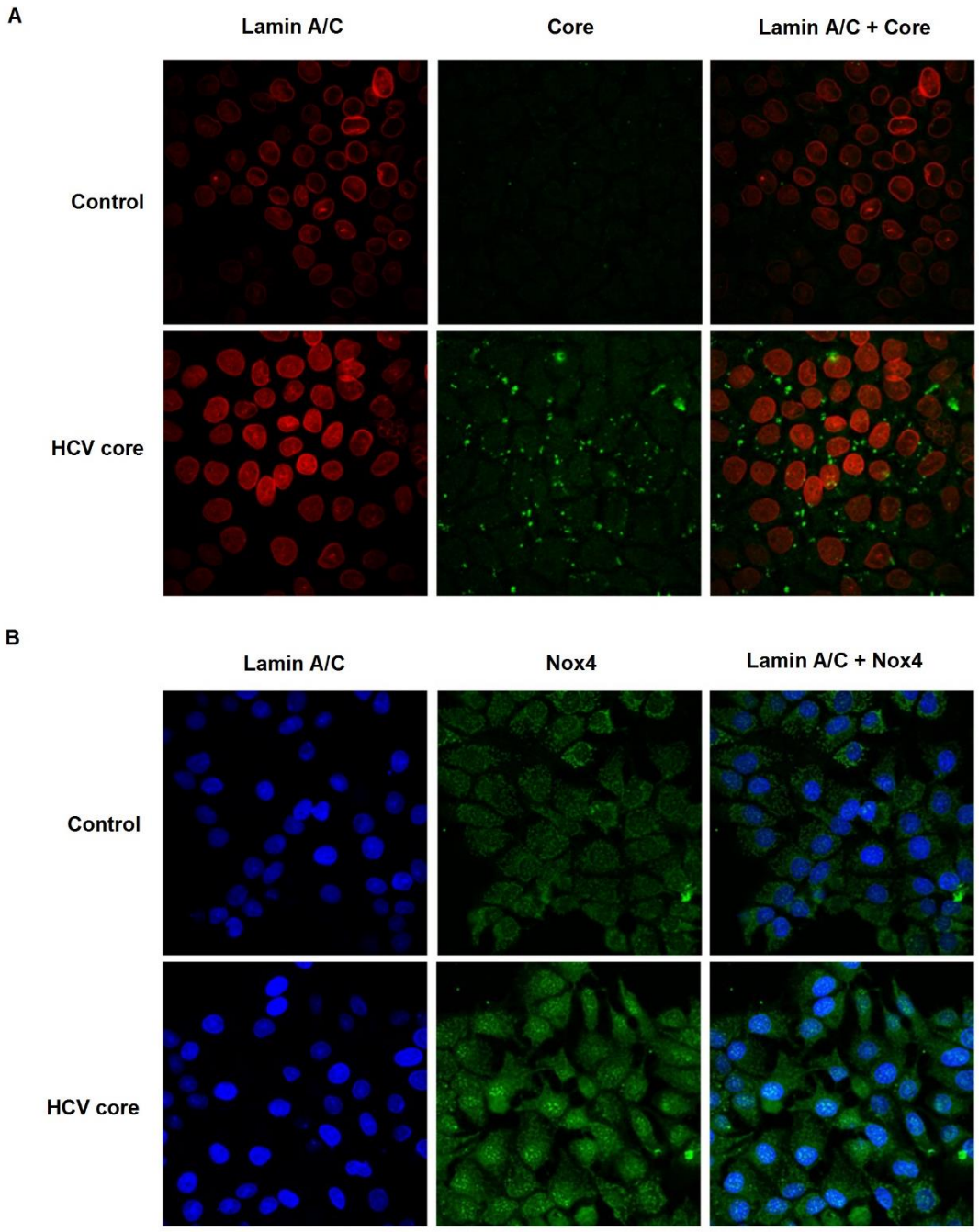

Figure 4. Immunofluorescence detection of core and Nox4 proteins in hepatocytes stably expressing HCV core. FITC-conjugated antibodies were excited by a 488nm laser with emission detected at 515±30nm. Alexa Fluor® 555-conjugated antibodies (Life Technologies) excited at 543nm with emission detected at 590±50nm. TRITC-conjugated antibodies (Santa Cruz Biotechnology) were excited at 543nm with emission detection at 650LP. Mouse lamin A/C (Santa Cruz Biotechnology) was used to identify the nucleus. All slides were viewed at 600x magnification with the same laser intensity for corresponding samples. (A) HCV core localization in Huh-7 cells fixed with 1:1 methanol-acetone. Core was detected using rabbit core antibody (Abcam). (B) Nox4 localization in Huh-7 cells fixed with 1:1 methanol-acetone. Nox4 was detected by rabbit Nox4 antibody (EMD Millipore).

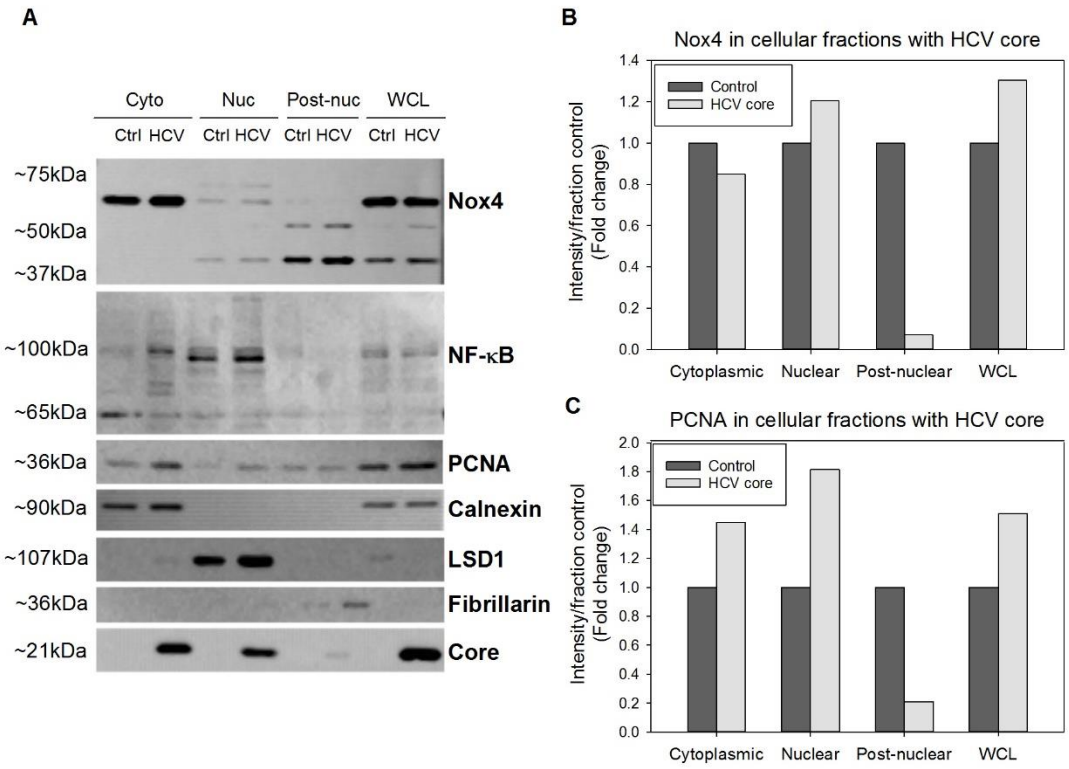

Figure 5. Characterization of subcellular fractions and whole cell lysates from stable hepatocytes expressing core. (A) Western blotting of subcellular fractions and whole cell lysates from Huh-7 cells with and without expressing core (n=1). For the cytoplasmic and nuclear fractions, 10µg of protein was loaded per well, and equal volume of post-nuclear fraction and whole cell lysate (both solubilized in 2x Laemmli buffer) were used for core and control samples. Calnexin was used as a marker for the cytoplasmic fractions and WCL, LSD1 was used as a nuclear marker, and fibrillarin was intended to be used as a nucleolar marker. (B) Nox4 levels were calculated using the 67kDa band as it was present in all fractions in addition to the WCL. Intensities were normalized to the respective fractionation markers, and fold changes were determined with reference to corresponding control samples. (C) PCNA expression was assessed by semi-quantitative densitometry in a manner similar to that of Nox4.

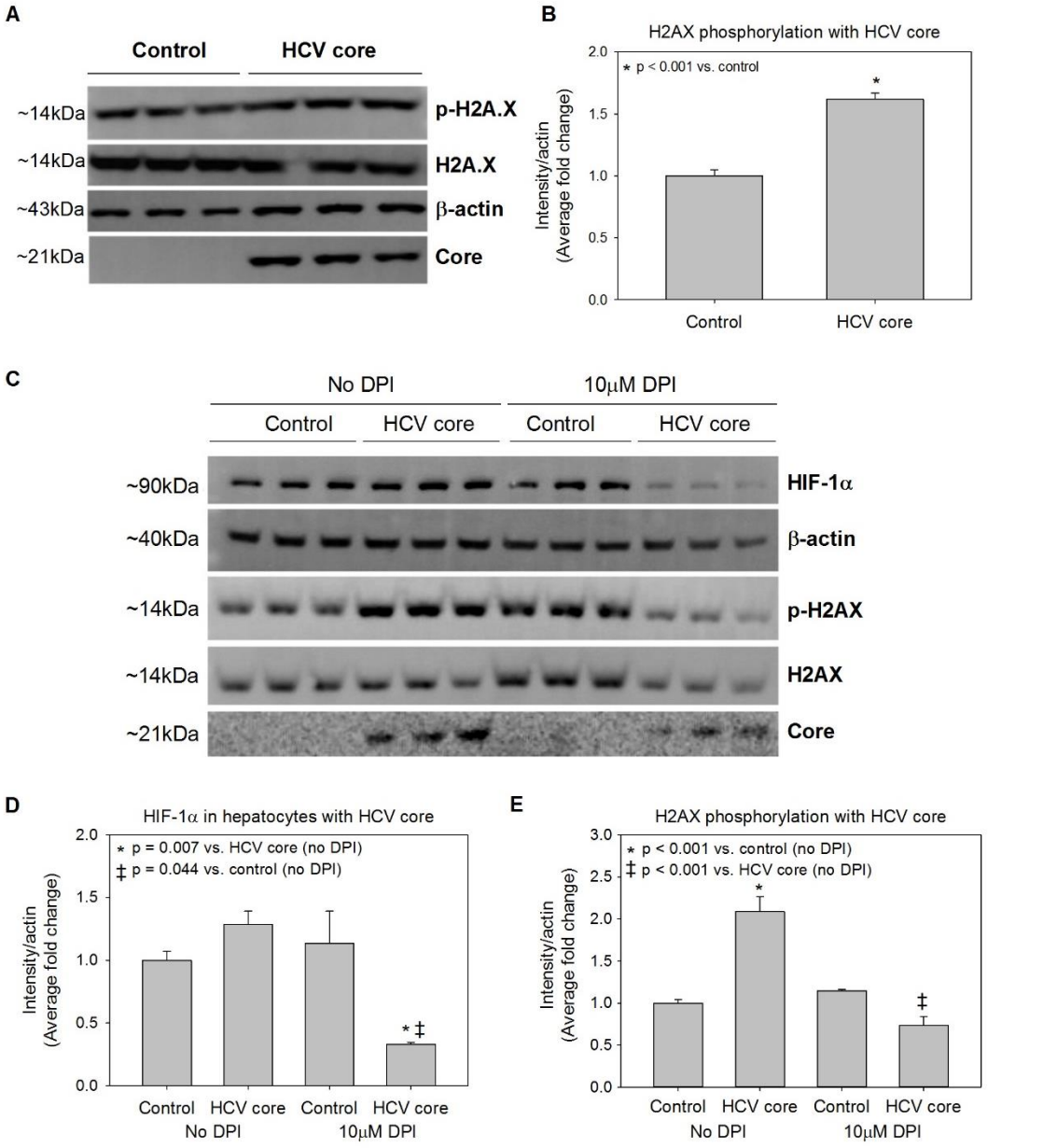

Figure 6. DNA damage markers in stable hepatocytes expressing core. All DPI treatments were conducted for 60 minutes followed by collection and processing for Western Blotting, and experiments were performed in triplicates. Phosphatase inhibitors were used during cell collection and processing to obtain lysates. No DPI-treated cells were administered an equal volume of water as a solvent. (A and B) Western Blotting and densitometry analysis of H2A.X-γ/H2A.X in hepatocytes constitutively expressing core. Intensities of H2A.X-γ and H2A.X were normalized to respective levels of β-actin before the ratio was determined. (C) Western Blotting of stable core-expressing cells treated with DPI at a final concentration of 10μM. Samples were processed in the same manner as described above. (D) HIF-1α levels were assessed by densitometry with normalization to β-actin. (E) Ratio of H2A.X-γ/H2A.X was assessed as described above. Average fold change was calculated with respect to control cells treated with solvent.

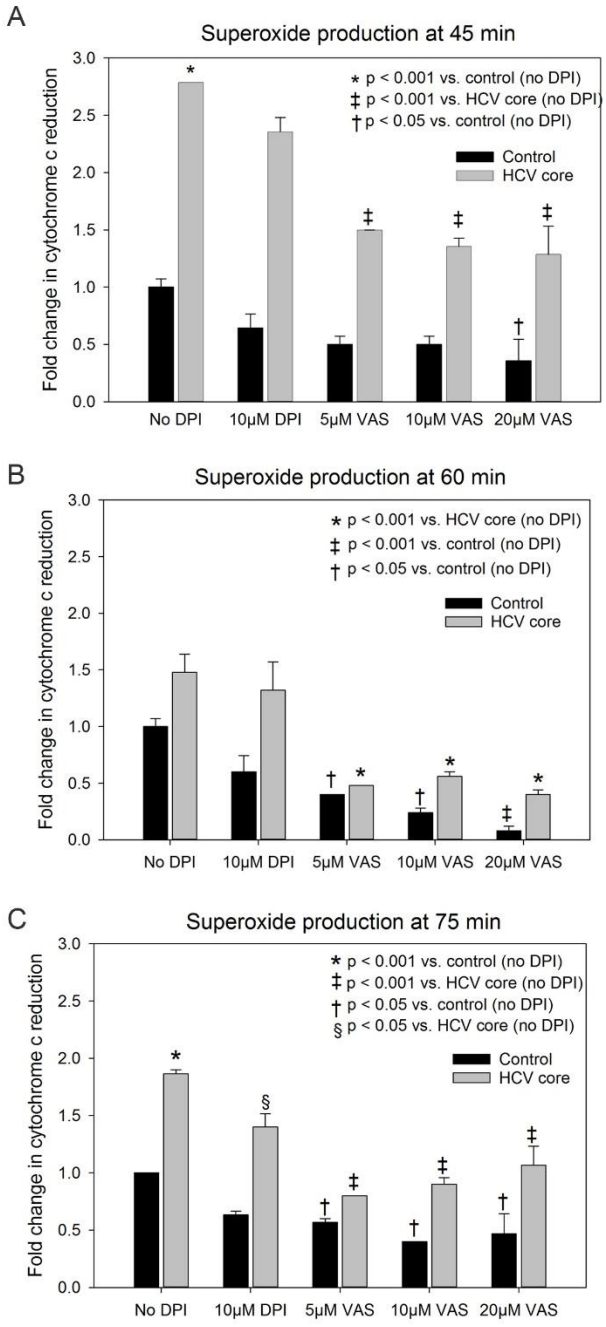

Figure 7. Nox activity is diminished in lysed hepatocytes treated with the novel Nox inhibitor, VAS-2870. Enzyme activity was measured by SOD-inhibitable cytochrome c reduction in lysed hepatocytes treated with varying final concentrations of Nox-specific VAS-2870 (Enzo Life Sciences) inhibitor. Lysis was achieved by sonication of cell pellets in ICLB with protease inhibitors, all performed on ice. Equal concentrations of protein, determined by BCA assay, were used for each sample (n=3). Absorbance was measured at 550nm with a reference at 540nm. (A) Cytochrome c reduction measured after a 45 minute reaction. (B) Cytochrome c reduction after an additional 15 minutes of reaction time, corresponding to 60 minutes. (C) Cytochrome c reduction 30 minutes after the initial reaction measurement, for a total reaction time of 75 minutes.